UNIVERSIDAD NACIONAL AUTÓNOMA DE MÉXICO
PROGRAMA DE POSGRADO EN ASTROFÍSICA

Instituto de Astronomía

LÍMITES A LA MASA DE LOS PERTURBADORES MASIVOS (MACHOS) A PARTIR DE LAS BINARIAS ABIERTAS DEL HALO GALÁCTICO.

TESIS

PARA OPTAR POR EL GRADO DE
DOCTOR EN CIENCIAS (ASTROFÍSICA)

PRESENTA
MIGUEL ANGEL MONROY RODRÍGUEZ

TUTOR
M EN C. CHRISTINE PATRICIA ALLEN ARMIÑO,
INSTITUTO DE ASTRONOMÍA

MÉXICO, D. F. DICIEMBRE 2013

INDICE

I. Introducción general

En el presente trabajo de tesis abordamos dos problemas relativamente independientes. El primero consiste en la elaboración de un catálogo extendido de binarias abiertas del halo galáctico, el cual intenta superar en varios aspectos a los catálogos existentes en la actualidad. El segundo problema consiste en la aplicación del nuevo catálogo para elaborar un modelo dinámico de la evolución de las binarias abiertas del halo con el objeto de establecer cotas a la masa de los perturbadores masivos (MACHOs por sus siglas en inglés: *Massive Compact Halo Objects*).

Las binarias abiertas son objetos dinámicamente muy frágiles, pues están débilmente ligadas y sujetas a perturbaciones por otras estrellas, por los brazos espirales de la Galaxia, por su mismo paso por el disco galáctico, por efectos de la marea galáctica, por encuentros con nubes moleculares, y por encuentros con otros posibles perturbadores, especialmente los MACHOs en el halo galáctico. Por esta razón, pueden ser utilizados como sensores para determinar las propiedades de los perturbadores. En el caso particular de las binarias abiertas del halo, puesto que pasan la mayor parte del tiempo en regiones con baja densidad, puede esperarse que se conserven la distribución original de sus separaciones o semiejes mayores durante más tiempo que las binarias del disco galáctico.

La función de distribución de los semiejes mayores de las binarias, al ser un reflejo directo de la distribución de la energía de amarre de estos sistemas, ha sido utilizada para modelar la evolución dinámica de las binarias sujetas a diversos tipos de perturbaciones (Weinberg, Shapiro & Wasserman 1987, Wasserman & Weinberg 1991, Yoo, Chanamé & Gould 2004, Jian & Tremaine 2010). con el paso del tiempo, el efecto de las perturbaciones tenderá a disolver paulatinamente las binarias más abiertas. Así, por ejemplo, Weinberg et al. (1987), Wasserman & Weinberg (1991, y más recientemente Jiang & Tremaine (2010) han estudiado la evolución de las binarias abiertas del disco galáctico sujetas a perturbaciones por estrellas y por nubes moleculares. Tanto Weinberg como Wasserman & Weinberg encontraron que la marea galáctica no afecta a las binarias con separaciones menores que 0.65 pc, y por tanto, no la tomaron en cuenta en sus modelos. En cambio, Jiang & Tremaine (2010) si encontraron efectos de marea para sus binarias más abiertas, con separaciones mayores que 100,000 AU. En todo caso, incluso las binarias más abiertas de nuestro catálogo no llegan a esos límites y pueden considerarse estables frente a los efectos de la marea galáctica.

En trabajos anteriores, la función de distribución de las separaciones (o semiejes) de las binarias abiertas ha sido objeto de controversia. Así, está muy difundida en la literatura la distribución de Duquennoy & Mayor (1991) que tiene una forma Gaussiana en el logaritmo de los períodos. Es de notarse que esta distribución fue originalmente propuesta por Kuiper (1935) y ha sido recientemente actualizada por Raghavan et al. (2010). Una distribución Gaussiana para los logaritmos de los periodos, abarcando desde las binarias más estrechas (espectroscópicas y/o eclipsantes) hasta las más abiertas (binarias visuales y binarias de movimiento propio común) sugeriría un mismo mecanismo de formación para todos estos tipos, lo cual es muy poco plausible. Los escenarios de formación más plausibles para la formación de binarias abiertas son: disolución de sistemas múltiples (Reipurth & Mikkola 2012), la captura de estrellas durante la disolución de cúmulos (Kouwenhoven et al. 2010, Moeckel & Clarke 2011, Perets & Kouwenhoven 2012) y la sugerencia de que estas prevalecen a la disolución de cúmulos o estructuras acretadas en el halo galáctico (Allen & Poveda 2007). La distribución de los cocientes de masa de ambas componentes de las binarias tampoco apoya un origen común para todas las binarias, pues parece ser muy distinta en el caso de las binarias estrechas (ambas componentes tienden a tener masas iguales) que en el caso de las binarias abiertas (ambas componentes tienen masas que se distribuyen de acuerdo a la función de Salpeter, esto es, las masas de las secundarias tienden a ser mucho mas pequeñas que las de las primarias). En nuestro estudio, nos concentraremos en las binarias abiertas, es decir, en aquellas que están situadas a separaciones mayores que las que corresponden al máximo de la distribución de Duquennoy & Mayor, es decir, en aquellas con semiejes mayores de más de aproximadamente 100 AU.

Incluso en el caso de las binarias abiertas, la función de distribución de las separaciones es controversial. Algunos autores (Chanamé & Gould 2004, Quinn et al. 2009) han propuesto que esta distribución sigue una ley de potencias con exponentes que varían entre -1.0 (Sesar et al. 2008, Lepine & Bongiorno 2007) hasta -1.55 (Chanamé & Gould para sus binarias del halo) o 1.67 (ibid, para binarias del disco). Poveda et al. (1994, 1997, 2003, 2004) encuentran un exponente -1, pero hasta distintos valores límite del semieje máximo, más allá del cual la distribución se ve mermada por efectos disolutivos. Estos valores límite de los semiejes dependen de la edad del grupo estudiado, y son mayores mientras más jóvenes son las binarias. Allen et al. (2000) al estudiar binarias del halo, también encuentran un valor de -1 para el exponente, pero hasta distintos valores límite del semieje, tanto mayores cuanto menores son los tiempos que las binarias pasan en el disco.

En vista de lo controversial que ha resultado la distribución de semiejes de las binarias abiertas, y de la importancia que el tema tiene para los modelos dinámicos de la evolución de estos sistemas, así como para entender mejor su origen, hemos dedicado un especial interés al estudio de la distribución de los semiejes de las binarias contenidas en el catálogo mejorado de binarias del halo. Se han sometido diversas muestras de binarias a la prueba de Kolmogorov-Smirnov, y hemos podido demostrar que la función de distribución de las separaciones (o semiejes) sigue, en efecto, una ley de potencias con exponente -1, relación de Oepik (Oepik 1994).

$$f(s) \propto s^{-1} \qquad (1)$$

donde s representa la separación de las binarias, esta relación es válida tanto para las separaciones angulares ($s = \theta$) como para los semiejes mayores esperados $\langle a \rangle$. Además, hemos obtenido con precisión los valores del semieje hasta los cuales la relación es válida, valores que nuevamente resultan mayores cuanto menos tiempo pasan las binarias en el disco galáctico. Estos resultados están contenidos en el primer artículo (que ya fue aceptado para ser publicado en el Astrophysical Journal).

En el segundo problema abordado en este trabajo de tesis, se emplean los datos contenidos en el catálogo ampliado de binarias abiertas del halo para establecer límites a las masas máximas de los perturbadores masivos del halo.

Anteriormente, Yoo et al. (2004) habían utilizado 90 binarias abiertas del halo, provenientes del catálogo de Chanamé & Gould (2004) para establecer como masa máxima posible para los MACHOs una valor de 43 $M_{\odot}$. Este límite dejaba abierto un intervalo muy pequeño para los posibles valores de las masas de estos perturbadores, pues los experimentos de microlentes (Tisserand et al. 2007, Wyrzykowski et al. 2008) establecían que los MACHOs podían tener masas de cuando mucho 30 $M_{\odot}$. Otros trabajos basadosn en la estabilidad del disco galáctico solo podían descartar MACHOs de masas mayores a 10^6 $M_{\odot}$ (Lacey & Ostriker 1985, Rujula et al. 1992).

Algunos años después, Quinn et al. (2009) estudiaron las velocidades radiales de cuatro de las binarias más abiertas de Yoo et al. (2004), y encontraron valores concordantes para tres de ellas; sin embargo, la cuarta resultó ser una falsa binaria, es decir, la coincidencia al azar de la posición de dos estrellas sobre la bóveda celeste, situadas a distintas distancias de nosotros, y casualmente mostrando los mismos movimientos propios. Al suprimir esta binaria de la muestra, y al corregir un error en la definición de los intervalos de confianza de los ajustes empleados por Yoo et al. (2004) el límite para la

masa de los MACHOs aumenta hasta unas 500 $M_{\odot}$. Quinn et al. (2009) concluyeron que la muestra de binarias del halo disponible no es lo suficientemente extensa para establecer límites confiables a la masa de los MACHOs.

Esta situación nos llevó a elaborar el catálogo descrito con más detalle en la siguiente sección. En el nuevo catálogo, y gracias a la integración numérica de las órbitas galácticas, se determinan los tiempos que cada binaria pasa en el disco de la galaxia. Este parámetro resulta ser crucial para los modelos de la evolución dinámica de estos objetos, puesto que en el disco ocurren las perturbaciones más importantes, debidas a encuentros con estrellas, brazos espirales y nubes moleculares. Además, pudimos establecer que 9 de las binarias más abiertas –que son especialmente frágiles, y por ende, sensibles a las perturbaciones– contaban con observaciones de velocidades radiales para ambas componentes, y que éstas concordaban dentro de la incertidumbre observacional; con ello, queda prácticamente asegurada la naturaleza física de estos objetos (es decir, que son estrellas ligadas gravitacionalmente y no solamente binarias ópticas).

A continuación, y siguiendo la metodología de Yoo et al. (2004) desarrollamos un modelo tipo Monte Carlo para la evolución dinámica de un conjunto de 100 000 binarias virtuales y aplicamos este modelo a varias sub-muestras de binarias de nuestro catálogo, ordenadas según el tiempo que pasan en el disco galáctico, También tomamos en cuenta que la densidad del halo no es constante, como lo habían supuesto Yoo et al. (2004) El resultado de nuestros modelos dinámicos nos permite establecer como masa máxima para los MACHOS del halo galáctico un valor de 11-15 $M_{\odot}$. Este límite es menor que el obtenido por Yoo et al. (2004) y en combinación con los resultados de las observaciones de microlentes, prácticamente excluye la existencia de perturbadores masivos en el halo galáctico. El artículo que contiene los resultados de los modelos dinámicos fue enviado al Astrophysical Journal, y se encuentra actualmente en revisión.

II. Introducción al trabajo: "An improved catalog of halo wide binary candidates"

II.1. Importancia de las Binarias Abiertas.

Las binarias abiertas tanto del disco como del halo galáctico son importantes para entender los procesos de formación estelar y la evolución dinámica. Las binarias más abiertas son muy frágiles y fáciles de destruir por encuentros con perturbadores de todo tipo (estrellas, nubes moleculares, brazos espirales, mareas galácticas o posibles MACHOs). Esta es la razón por la cual han sido utilizadas como sensores para establecer las propiedades de dichos perturbadores (Weinberg, Shapiro & Wasserman 1987, Wasserman & Weinberg 1991, Yoo, Chanamé y Gould 2004, Jian & Tremaine 2010, entre otros).

En particular, las propiedades orbitales de las binarias abiertas en el halo galáctico permanecen prácticamente sin cambio desde su formación excepto por los efectos de su interacción gravitacional durante encuentros con posibles perturbadores masivos del halo de la Galaxia, encuentros que suceden a lo largo de la trayectoria galáctica de las binarias .

Para nuestros propósitos, consideraremos que una binaria es "abierta" cuando su semieje es mayor que aproximadamente 100 AU. Estas binarias se encuentran, consecuentemente, después del máximo de la distribución de separaciones encontrada por Duquennoy & Mayor (1991). Hay muchas razones para suponer que los mecanismos de formación para las binarias abiertas son distintos de aquellos válidos para las binarias cerradas. Nuestro estudio se restringe a las binarias abiertas, en particular, a las pertenecientes al halo galáctico.

II.2. Construcción del catálogo mejorado.

Existen en la literatura varios catálogos de binarias abiertas del halo, entre los cuales los más empleados han sido el de Allen et al. (2000) y el de Chanamé & Gould (2004). El primero contiene 76 binarias del halo, y proporciona órbitas galácticas para la mayoría de ellas. El segundo contiene 90 binarias atribuidas al halo, aunque no cuenta con órbitas galácticas, la pertenencia al halo se infiere a partir de su posición en el diagrama de Movimiento Propio Reducido (RPM por sus siglas en inglés: *Reduced Proper Motion*).

Para la construcción del nuevo catálogo hicimos una revisión exhaustiva de la literatura para generar una lista de inicial de candidatos. El principal método de detección para este tipo de binarias son sus movimientos propios, que deben ser paralelos e iguales en magnitud. En consecuencia, la mayor parte de estas binarias proviene de los catálogos de movimientos propios de Luyten (1979), y de su revisión por Gould & Salim (2003), Salim & Gould (2003), así como Chanamé & Gould (2004). Además, incorporamos algunas binarias de las listas de Ryan (1992), Zapatero-Osorio & Martín (2004), y algunos otros autores, quienes realizaron estudios espectroscópicos generalmente restringidos a las primarias de estos objetos.

El nuevo catálogo incluye 111 candidatos a binarias del halo provenientes de Allen et al. (2000), 110 de Chanamé & Gould (2004), 23 de Zapatero-Osorio & Martín (2004), y 7 de Ryan (1992), para darnos un total de 251 sistemas.

II.3. Movimientos Propios Comunes.

Los movimientos propios de nuestra lista inicial de candidatos fueron revisados utilizando la base de datos astronómica Simbad, para comprobar que, en efecto, fueran iguales y paralelos. De esta manera, pudimos eliminar varios candidatos. A manera de ilustración, mostramos en las Figuras 1 a 4 (no incluídas en el artículo) algunas de nuestras binarias de movimiento propio común.

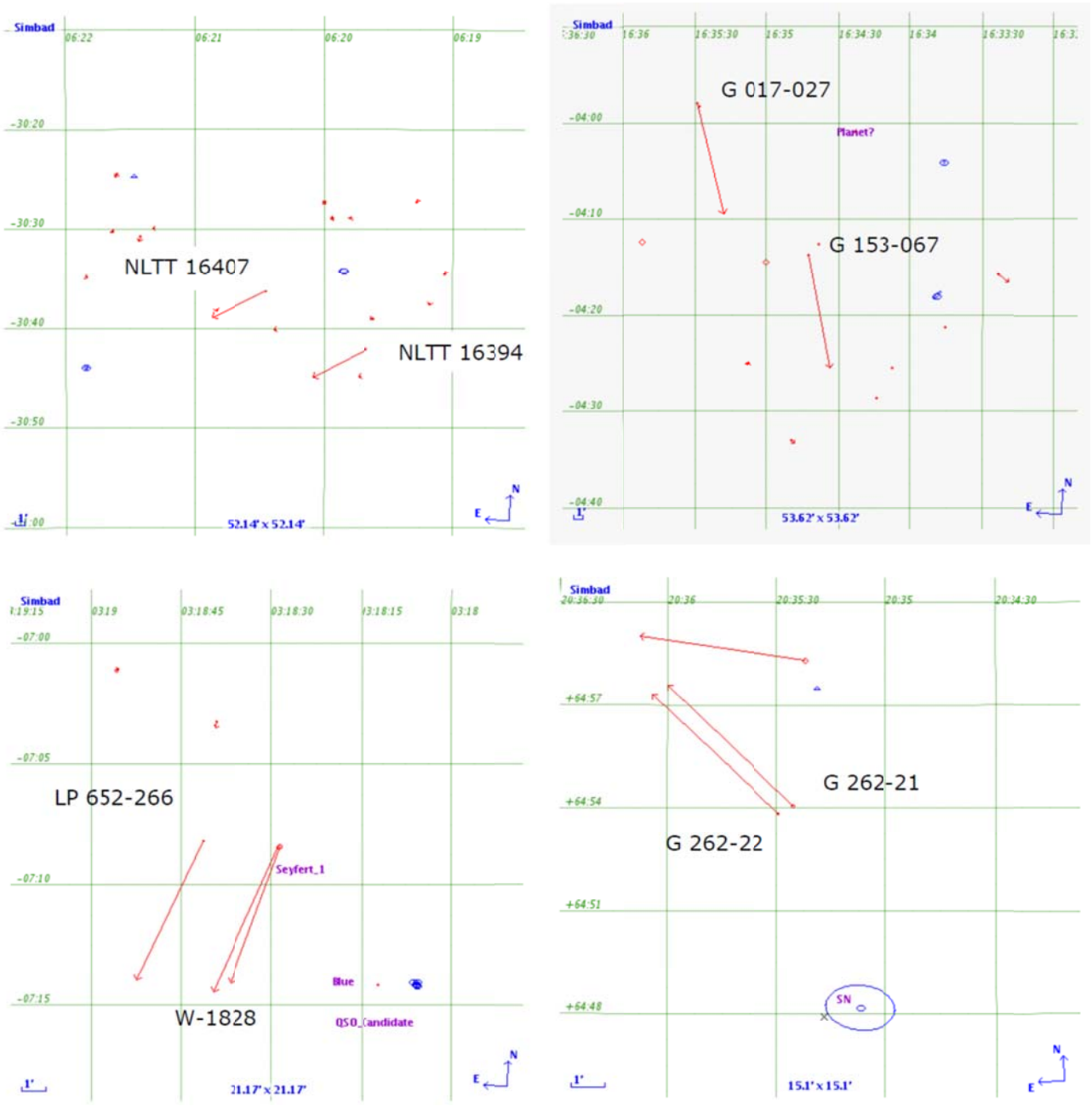

Figuras 1 a 4 de movimientos propios comunes para algunas de las binarias de nuestro catalogo.

II.4. Diagrama de Movimiento Propio Reducido.

A continuación, construimos un diagrama RPM e intentamos distinguir por este medio los verdaderos objetos del halo, siguiendo el método propuesto por Chanamé & Gould (2004), (véase la Fig. 1 del artículo). Sin embargo, encontramos que la línea de separación propuesta por estos autores no resultaba muy satisfactoria, pues dejaba fuera del halo un buen número de binarias cuyas órbitas galácticas (calculadas en Allen et al. 2000) mostraban su clara pertenencia al halo. Propusimos

entonces una nueva línea de separación, para incluir a estas binarias como candidatos. Además, excluimos 40 binarias cuyas órbitas, independientemente de su posición en el diagrama RPM, demostraban su clara pertenencia al disco, con lo cual obtuvimos una lista, más depurada, con 212 binarias.

II.5. Propiedades dinámicas de las binarias de nuestro catálogo.

El siguiente paso fue buscar en la literatura velocidades radiales para nuestra lista depurada de candidatos. Encontramos que 150 de ellos contaban con datos para las velocidades radiales, y 9 de ellas tenían velocidades radiales publicadas para ambas componentes del par, y los valores eran concordantes dentro de las incertidumbres observacionales publicadas. Esto último da prácticamente la certeza de que se trata de sistemas físicamente ligados, y no de la asociación al azar de dos estrellas de campo.

A continuación, se calcularon las órbitas galácticas de las 150 binarias con datos suficientes. Para ello, usamos el potencial galáctico de Allen & Santillán (1991) para integrar las órbitas hacia atrás en el tiempo durante 13 Giga-años. Estas órbitas nos permiten calcular el tiempo que pasa cada binaria dentro del disco galáctico ($|z| < 500$ pc), y con ello contar con un parámetro muy importante para los modelos dinámicos. En vez de utilizar criterios fotométricos o espectroscópicos para cerciorarnos de la pertenencia de una binaria al halo, ahora usamos el tiempo que pasa en éste a lo largo de su recorrido galáctico. Las órbitas nos permiten ordenar a las binarias de acuerdo con la fracción de sus vidas que transcurre en el disco (o en el halo) de la Galaxia.

El catálogo final contiene un total de 251 candidatos a binarias del halo, para 150 de las cuales tenemos órbitas galácticas. La lista completa se proporciona en la Tabla 1 del artículo, en el cual también pueden encontrarse las definiciones de las columnas.

Las distancias listadas fueron tomadas del catálogo Hipparcos, cuando los errores relativos en las paralajes no excedían el 15%. Si los errores eran mayores, preferimos las distancias determinadas mediante la fotometría Stromgren de Nissen & Schuster (1991), o las calculadas mediante el polinomio de Chanamé & Gould (2004), usando su fotometría. Para algunas estrellas fue necesario adoptar las distancias obtenidas por medios espectroscópicos por Ryan (1992) o Zapatero-Osorio & Martín (2004).
2.4 brillo las binarias

Las magnitudes absolutas de las primarias se calcularon a partir de las distancias y de las magnitudes visuales aparentes dadas por los observadores. Las magnitudes visuales absolutas de las secundarias se calcularon siguiendo el método dado en Allen et al. (2000), a partir de las fotometría precisa de las primarias y de la diferencia de magnitudes entre las primarias y las secundarias, en dos colores. Para las binarias procedentes de Chanamé & Gould (2004), se adoptaron los datos fotométricos de estos autores.

II.5 Función de distribución de separaciones y evolución dinámica de una muestra de binarias.

Las separaciones lineales entre las componentes se calcularon a partir de las separaciones angulares y las distancias. Los semiejes mayores esperados se calcularon a partir de las separaciones observadas mediante la fórmula teórica de Couteau (1960)

$$\langle a \rangle (UA) = \frac{1.4}{\pi} \cdot s'' \qquad (2)$$

Donde el semieje mayor esperado $\langle a \rangle$ es proporcional a la separación angular proyectada s.

Como se puede ver en las figuras del artículo, se estudiaron las principales propiedades estadísticas de la muestra de 251 candidatos a binarias abiertas del halo, a saber:

(a) la distribución de las magnitudes absolutas de las primarias y de las secundarias (Figura 2).

(b) la distribución de velocidades peculiares (Figura 3), la cual nos confirma que la muestra contiene un número considerable de verdaderas estrellas del halo, y

(c) la distribución de separaciones angulares y semiejes esperados, la cual nos permitió establecer los resultados más importantes de nuestro estudio.

En vista de la importancia que tiene la distribución de semiejes para los modelos dinámicos de la evolución de las binarias, y dado que este ha sido un tema de mucha controversia en la literatura, dedicamos un esfuerzo especial al estudio de esta distribución para distintos grupos de binarias extraídas del catálogo.

La validez de la relación de Oepik (que como hemos mencionado, es un ajuste a la función de distribución de separaciones tipo ley de potencias con exponente -1) ha sido demostrada para muchas muestras independientes de binarias abiertas (Allen et al. 1997, Sesar et al. 2008, Lepine & Bongiorno 2007, Allen et al. 2000). Su validez fue establecida por Poveda & Allen (2004) y Poveda et al. (2007) para muestras de binarias de distintas edades, pero hasta semiejes límite que son función de la edad del grupo, lo cual es justamente lo esperado a partir de consideraciones dinámicas Valtonen (1997). Resultó ser válida también para una muestra de binarias completa en un volumen de 10 pc estudiada por Poveda & Allen (2004) y Poveda (2007), lo cual demuestra que su validez no se ve afectada por posibles incompleteces o sesgos en las muestras. Para las binarias del nuevo catálogo, encontramos que la relación de Oepik es válida tanto para las separaciones angulares como para los semiejes esperados. También demostramos que distintos sub-grupos siguen esta relación hasta distintos valores del semieje.

Por otra parte, hay razones para suponer que la relación de Oepik representa la distribución primigenia de separaciones, puesto que ha sido encontrada para grupos muy jóvenes, que aún no han sufrido perturbaciones de consideración (Poveda & Hernández-Alcántara 2003, Poveda et al. 2007). También existen razones teóricas que apoyan su validez. Así, Valtonen (1997) ha mostrado que dicha distribución corresponde a una situación de equilibrio dinámico. Debemos enfatizar que hemos demostrado su validez incluso para las binarias del disco y del halo galáctico estudiadas por Chanamé & Gould (2004), para las cuales estos autores proponen una distribución según una ley de potencias con exponentes distintos de -1. Para las primeras, estos autores encontraron un exponente de -1.67, pero con un "aplanamiento" hacia las separaciones pequeñas que no pudieron explicar. Para las segundas el exponente que encontraron fue de -1.55. Nuestras pruebas de Kolmogorov-Smirnov demuestran contundentemente que ambos grupos obedecen la relación de Oepik, las binarias atribuidas al halo hasta separaciones de 63" (97 de sus 110 binarias), las del disco para separaciones 10"< s <36" (285 de sus 523 binarias). En este último caso, la distribución a separaciones mayores que 36" muestra el cambio de pendiente esperado debido a la disolución de los sistemas más separados, que va despoblando paulatinamente esta parte de la distribución.

Los principales resultados que se obtuvieron del estudio de la distribución de separaciones y semiejes esperados para las binarias del nuevo catálogo se describe a continuación. Las figuras pueden encontrarse en el artículo que anexamos.

La distribución acumulada de separaciones angulares de la muestra completa de 251 binarias se muestra en la Figura 4 del artículo. La línea recta es un ajuste tipo Oepik a la distribución de separaciones angulares. En la Figura 5 se muestra la distribución de semiejes esperados, con el mismo ajuste. Vemos que el ajuste a la distribución de Oepik es una buena representación también de esta muestra. Lo mismo encontramos para varias sub-muestras. Entre ellas, la lista depurada de 211 candidatos (Figura 8), la lista de 150 binarias con órbitas galácticas calculadas (Figura 14) , y finalmente la lista de las 50 binarias que menos tiempo pasan en el halo (Figura 16), y la de aquellas que más tiempo pasan en el halo (Figura 17). Todas estas muestras se sometieron a la prueba de Kolmogorov-Smirnov, para evaluar la probabilidad de que procedan de una distribución tipo Oepik. El resultado de estas pruebas se muestra en las Figuras 10,15, 18 y 19. En todos los casos pudo demostrarse que la distribución de Oepik era válida, si bien hasta valores de la separación (o del semieje esperado) distintos. Así, para la muestra depurada de 211 candidatos, la distribución de Oepik es válida hasta un valor del semieje esperado de 25,000 AU (Figura 10); para las 150 binarias con órbitas galácticas calculadas es válida hasta un semieje esperado de 28,000 AU (Figura 15); para las 50 binarias que pasan más tiempo en el disco, es válida hasta un semieje esperado de 15,000 AU (Figura 18); mientras que para las 50 binarias que pasan más tiempo en el halo es válida hasta un semieje esperado de 63 000 AU (Figura 19). Para efectos de comparación, mencionamos que el grupo de 50 binarias del catálogo de Allen et al. (2000) que más tiempo pasan en el halo siguen la distribución de Oepik hasta un semieje esperado de 20 000 AU.

Estos resultados obtenidos en la primera parte de nuestro trabajo, confirman y refuerzan la idea de que la distribución primigenia de los semiejes de las binarias es de tipo Oepik, y que por efectos de las interacciones dinámicas, predominantemente del disco galáctico, la parte más abierta de la distribución se va disolviendo paulatinamente.

III. Carta de aceptación del trabajo en el Atrophysical Journal

Asunto: Acceptance for publication in The Astrophysical Journal:ApJ92060R1
Fecha: Mon, 12 Aug 2013 08:46:07 -0400
De: apj@msubmit.net
Responder a: bburton@nrao.edu , apjjournal@gmail.com
Para: chris@astro.unam.mx
CC: bburton@nrao.edu

August 12, 2013

Dr. Christine Allen
Universidad Nacional Autonoma de Mexico
Instituto de Astronomia
Avenida Universidad 3000
Mexico, Distrito Federal 04510
Mexico

Title: An Improved Catalog of Halo Wide Binary Candidates

Dear Dr. Allen,

I am happy to inform you that your revised manuscript is accepted for publication in The Astrophysical Journal.

In advising acceptance of the revised manuscript, your referee made the brief comments that I append below. These comments refer to corrections that should be made to your bibliography: I have also looked over the bibliography myself, and add a few additional minor notes. Rather than delay acceptance by asking you to submit a revision, I ask you to give these simple matters due attention during the proof-reading stage.

I am sending the accepted version to the ApJ editorial office. Correspondence concerning the logistical aspects of publishing this manuscript should be directed to apj@apj.usask.ca. If you have any additional questions concerning the scientific content of your manuscript, please direct them to me.

With best wishes,

Butler Burton

Prof. W. Butler Burton
Associate Editor-in-Chief, The Astrophysical Journal
Professor Emeritus, University of Leiden
National Radio Astronomy Observatory

IV. Contribuciones específicas del autor al artículo:

"An improved catalog of halo wide binary candidates"

por Miguel A. Monroy-Rodríguez & Christine Allen

(Aceptado para su publicación en The Astrophysical Journal.)

-Revisar y actualizar todos los datos de la Tabla 1, empleando la base de datos Simbad

-Construir el diagrama RPM, Figura1.

-Buscar y elegir las mejores magnitudes para las componentes de las binarias

-Calcular, mediante el polinomio propuesto por Chanamé & Gould (2004) y las mejores magnitudes, las distancias a las binarias.

-Elaborar y probar el programa que calcula la prueba de Kolmogorov-Smirnov

-Someter a diversos grupos de binarias a la prueba de Kolmogorov-Smirnov, para establecer cuál es el mejor exponente para la ley de potencias de la distribución de separaciones o semiejes esperados, y cuál es la separación o semieje a partir de la cual la distribución se abate.

-Elaborar todas las gráficas

-Recopilar la bibliografía

An improved catalog of halo wide binary candidates

Miguel A. Monroy-Rodríguez [1] & Christine Allen [1]

Instituto de Astronomía, Universidad Nacional Autónoma de México, Apdo. Postal 70-264, México, D.F. 04510, México; chris@astro.unam.mx

ABSTRACT

We present an improved catalog of halo wide binaries, compiled from an extensive literature search. Most of our binaries stem from the common proper motion binary catalogs by (Allen et al. 2000), and (Chanamé & Gould 2004) but we have also included binaries from the lists of (Ryan 1992) and (Zapatero-Osorio & Matín 2004). All binaries were carefully checked and their distances and systemic radial velocities are included, when available. Probable membership to the halo population was tested by means of reduced proper motion diagrams for 251 candidate halo binaries. After eliminating obvious disk binaries we ended up with 211 probable halo binaries, for 150 of which radial velocities are available. We compute galactic orbits for these 150 binaries and calculate the time they spend within the galactic disk. Considering the full sample of 251 candidate halo binaries as well as several subsamples, we find that the distribution of angular separations (or expected major semiaxes) follows a power law $f(a) \sim a^{-1}$ (Oepik's relation) up to different limits (Oepik 1924). For the 50 most disk-like binaries, those that spend their entire lives within $z = \pm 500$ pc, this limit is found to be 19,000 AU (0.09 pc), while for the 50 most halo-like binaries, those that spend on average only 18% of their lives within $z = \pm 500$ pc, the limit is 63,000 AU (0.31 pc). In a companion paper we employ this catalog to establish limits on the masses of the halo massive perturbers (MACHOs).

Subject headings: binaries: general – catalogs – subdwarfs – Galaxy: halo

1. Introduction

Old disk and halo binaries are relevant to the understanding of processes of star formation and early dynamical evolution. In particular, the orbital properties of the wide binaries remain unchanged after their formation, except for the effects of the galactic tidal field or of their interaction with perturbing masses encountered during their lifetimes, as they travel in the galactic environment. The widest binaries are quite fragile and easily disrupted by encounters with various

perturbers, be they passing stars, molecular clouds, spiral arms, MACHOs (massive compact halo objects) or the galactic tidal field. In this way, they can be used as probes to establish the properties of such perturbers (Weinberg et al. 1987; Wasserman & Weinberg 1991; Yoo et al. 2004; Jiang & Tremaine 2010).

An interesting application of halo wide binaries was proposed by (Yoo et al. 2004) who used the catalog of (Chanamé & Gould 2004), hereinafter ChG, containing 116 halo binaries to try to detect the signature of disruptive effects of MACHOs in their widest binaries. They were able to constrain the masses of such perturbers to $m < 43\ M_{\odot}$, essentially excluding MACHOs from the galactic halo, since a lower limit of about 30 $M_{\odot}$ is found by other studies (Afonso et al. 2003; Alcock et al. 1998, 2001). However, as was shown a few years later by (Quinn et al. 2009), this result depends critically on the widest binaries of their sample, as well as on the observed distribution of the angular separations which, according to ChG, shows no discernible cutoff between 3.5″ and 900″. (Quinn et al. 2009) obtained radial velocities for both components of four of the widest binaries in the ChG catalog and found concordant values for three of them, thus establishing their physical nature. The fourth binary turned out to be optical, resulting from the random association of two unrelated stars. Excluding this spurious pair and assuming power law distributions with exponents between 0.8 and 1.6 for the observed separations they find a limit for the masses of the MACHOs of $m < 500\ M_{\odot}$, much less stringent than that found previously; they conclude rather pessimistically that the currently available wide binary sample is too small to place meaningful constraints on the MACHO masses. They also point out that the density of dark matter encountered by the binaries along their galactic orbits is variable, and that this variation has to be taken into account when calculating constraints on MACHO masses.

Motivated by these concerns, we have constructed a catalog of 251 candidate halo wide binaries. We describe the way the catalog was compiled in Section 2. In Section 3 we present some statistical properties for different subsamples of binaries, and examine the galactic orbits for the 150 binaries with sufficient observational data. Section 4 is devoted to a discussion of our results. We point out that for a total of 9 binaries concordant radial velocities for both components were found in the literature. A companion paper utilizes this catalog to dynamically model the evolution of wide halo binaries, and to obtain new limits on the MACHO masses.

We stress that our study pertains to the wide binaries only. The classical study of (Duquennoy & Mayor 1991) and its recent update (Raghavan et al. 2010) shows a log-normal distribution of periods. Our binaries correspond to the periods greater than the maximum period of these distributions, i.e. $P > 10^5$ yr, which corresponds approximately to semiaxes greater than 100 AU. For our present purpose, we use the term "wide binary" to refer to binaries with separations larger than that corresponding to the maximum in the Kuiper or Duquennoy-Mayor distribution, which are presumably formed by processes different from those responsible for the closer binaries.

2. Construction of the catalog

A search of the literature was conducted, looking for high velocity, metal-poor wide binaries, since such samples are likely to be rich in halo stars. Most of the binaries in the new catalog stem from the lists of (Ryan 1992; Allen et al. 2000; Chanamé & Gould 2004) and (Zapatero-Osorio & Matín 2004). All listed data were checked, and updated when necessary. We selected the most reliable data for the distances, metallicities and radial velocities. All proper motions were checked in the Simbad database and non-common proper motion companions were eliminated (i.e., we omitted pairs with proper motions differing by more than the published values). The catalog includes 111 halo binaries from (Allen et al. 2000), 110 halo binaries from (Chanamé & Gould 2004) 23 from (Zapatero-Osorio & Matín 2004) and 7 from (Ryan 1992), to give a total of 251 halo binary candidates.

In order to refine the sample, we constructed a reduced proper motion diagram (RPM), following (Salim & Gould 2003) and (Chanamé & Gould 2004). The RPM diagram for 251 candidate halo binaries is shown in Figure 1. The black diagonal line is the limit taken by ChG to separate disk from halo binaries. We note that this line excludes quite a few binaries for which galactic orbits from (Allen et al. 2000) clearly imply their halo membership. Therefore, we draw a new limit, indicated by the dotted line, which includes most of the (Allen et al. 2000) binaries with halo-like galactic orbits. Regardless of their position in the RPM diagram we exclude 40 binaries with galactic orbits such that they spend their whole lives within the disk, although their motions are clearly indicative of a thick disk or of an even dynamically hotter population. In this way, we end up with 212 binaries, most likely belonging to the galactic halo or thick disk.

To carry out the dynamical modelling of the evolution of halo binaries, the most useful quantity is the fraction of the lifetime that each binary spends far from the galactic disk. Thus, galactic orbits were calculated for all binaries with available radial velocities (at least for their primaries), a total of 150 systems. The (Allen & Santillán 1991) galactic potential was used, and the orbits were calculated backwards in time for 13 Gyr. This allowed us to compute for each system t_d/t, the fraction of time spent within $z = \pm 500$ pc.

The entire catalog is presented in Table 1. The entries are ordered by right ascension (J2000). Distances to the primaries were taken, when appropriate, from the Hipparcos catalog. Hipparcos distances were adopted for those stars with relative errors in their trigonometric parallaxes of less than 15%. For stars with larger errors, photometric distances were preferred, mostly taken from the lists of (Nissen & Schuster 1991) and references therein, or by means of the polynomial used by ChG, adopting their photometry. For a few stars not found in those lists, spectroscopically derived distances were taken from either (Ryan 1992) or (Zapatero-Osorio & Matín 2004). Thus, most of the binaries listed in the catalog should have errors of less than 15% in their adopted distances.

Absolute visual magnitudes for the primaries were calculated from the adopted distances and the apparent visual magnitudes given in the respective catalogs. Absolute magnitudes for the secondaries were calculated as described in (Allen et al. 2000) for their stars. They are mostly based on accurate photometry for the primary, and magnitude differences in two colors for the secondaries, a procedure which was shown by (Allen et al. 2000) to yield reliable values for the absolute magnitudes of the secondaries. For binaries stemming from (Chanamé & Gould 2004) their photometry was adopted. Secondaries from other sources are listed as in the original references.

Linear separations between the components were calculated from the angular separations and the adopted distances. The linear separations were transformed into expected values for the major semiaxes of the binaries by the statistical relation (Couteau 1960)

$$\langle a'' \rangle = 1.40 s''.$$

Therefore, a binary with projected angular separation s'' will have an expected major semiaxis $\langle a \rangle$ given by

$$\langle a \rangle (\mathrm{AU}) = \frac{1.40}{\pi} s''.$$

The above formula was derived by Couteau on theoretical grounds, assuming a random distribution of the geometrical elements of the orbit, as well as random times of passage through periastron. This relation turns out to be independent of the eccentricity distribution. Couteau also checked its observational validity based on more than 200 orbits, for which the constant turned out to be 1.411. A more recent empirical study (Bartkevičius 2008), based on data from the Catalog of Orbits of Visual Binary Stars (Hartkopf & Mason 2007) and the WDS (Mason et al. 2007), the result was $\log \langle a \rangle - \log s$ ranging from 0.112 to 0.102. In view of the large uncertainties of the empirically derived values, and to facilitate comparisons with previous work, we shall use Couteau's theoretical result.

In Table 1, we list in Column 1 the NLTT number of the primary, as well as the designation of its companion. In Column 2 we list alternative identifications of the primary. We provide, in order of preference, identifications in the Hipparcos, the HD, the Giclas (G) or the Wilson catalogs. Column 3 contains the identification of the secondary. Column 4 lists our best choice for the distance to the primary, as explained above. Columns 5 and 6 list the absolute magnitudes of the primary and secondary, respectively. Columns 7 and 8 the projected angular separation between the components and the expected value for the major semiaxis. The peculiar velocity of the binary is given in Column 9. This velocity is computed assuming a solar motion of (9, 12, 7) km s^{-1}. The radial velocity used to compute the peculiar velocity in Column 9 is taken from various sources,

listed mostly in the Simbad database. The presence of undetected close companions to one or both members of the binary will affect the radial velocities, and thus the computed orbits. The observers have, in general, taken care to detect variations due to unseen companions. But the stars are faint and metal-poor, and thus observationally difficult. For the orbit computations we checked the published radial velocities to make sure we were using the systemic radial velocity -when available. Otherwise, we checked for radial velocity variations in the published data, and excluded a few systems with widely discrepant values. Columns 10 to 12 contain the main orbital parameters of the galactic orbit; we list the apocentric distance $R_{\rm max}$, the maximum distance from the galactic plane $|z_{\rm max}|$ and the three-dimensional eccentricity e of the galactic orbit. In Column 13 we list t_d/t, the fraction of its lifetime the binary spends within the galactic disk ($z = \pm 500$ pc). In the last column, the provenance of the binary is given (A = Allen et al. 2000; CG = Chanamé & Gould 2004; Z = Zapatero-Osorio & Matín 2004; R = Ryan 1992).

3. Some statistical properties

3.1. The distribution of absolute magnitudes

Figure 2 shows the frequency distribution of the absolute magnitudes of the primaries (full line) and the secondaries (dotted line) of our catalog. Note particularly the extension to the faint end of the magnitudes of the secondaries. This constitutes a sampling of the faint end of the main sequence for these metal-poor and presumably old stars. Observationally, these secondaries are challenging objects, being faint and having only a few lines in their spectra, but undoubtedly they are interesting and worthy of being included in observational programs.

3.2. The distribution of peculiar velocities

Figure 3 is a histogram of the distribution of the peculiar velocities of the binaries. Note that most of the systems have peculiar velocities larger than 60 km s^{-1}, and thus can be considered to be good candidates to be bona fide thick disk or halo stars.

3.3. The distribution of angular separations and expected major semiaxes

Figure 4 shows the cumulative distribution of the angular separations of the full sample of 251 low-metallicity high-velocity binaries. The straight line is a fit to the Oepik distribution $f(s) = k/s$ (Oepik 1924). Figure 5 shows the same fit for the expected major semiaxes. In (Allen et al. 2000;

?), as well as here, we choose to display the distributions in cumulative form, since in this way we can apply directly the Kolmogorov-Smirnov (KS) test to quantitatively assess the probability that the observed distribution stems from a given theoretical distribution. Our choice of presentation of the angular distributions was criticized by ChG, who found a different exponent for the power law of their angular distributions. Since the matter remains controversial, we present below a brief discussion of the issue.

In Figure 6 we show the cumulative distribution of the ChG sample of 110 halo binaries. The straight line represents Oepik's distribution, corresponding to a power-law exponent of -1. In Figure 7 we show the result of applying the Kolmogorov-Smirnov test to this sample. It is obvious that Oepik's distribution shows an excellent fit to these stars up to an angular separation of 63 arc seconds, which includes 97 out of their 110 stars, leaving out those with the largest separations. We have performed the same test using an exponent of -1.6, as ChG do, and find a good fit, but only for binaries with separations larger than 3 arc seconds (94 binaries). Thus, it would appear that this controversy cannot be settled merely by goodness-of fit arguments. We would interpret the departure from Oepik's distribution as due to dynamical effects, an interpretation supported both from theoretical studies (Valtonen 1997 showed Oepik's distribution to correspond to dynamical equilibrium) and from the observed distributions found for many independent samples of stars, and for groups of different ages (Poveda et al. 2007; Sesar et al. 2008; Lépine & Bongiorno 2007; Allen et al. 2000). We think the Oepik distribution is to be preferred for the following reasons.

1. It has been shown to hold for many different samples of wide binaries ($a \geq 100$ AU) stemming from different and independent sources (Poveda et al. 2007; Sesar et al. 2008; Lépine & Bongiorno 2007; Allen et al. 2000). We show below that both the angular separations and the expected semiaxes of the candidate halo binaries in our improved catalog follow Oepik's distribution. We also show that different subgroups of the catalog also follow Oepik's distribution up to different limiting semiaxes.

2. It has been shown to hold up to different limiting separations for wide binaries of different ages (Poveda & Allen 2004; Poveda et al. 2007) which is exactly what one would expect from dynamical considerations.

3. It holds for a volume-complete sample of nearby wide binaries (Poveda & Allen 2004; Poveda et al. 2007) in the interval 133 AU $< a <$ 2640 AU.

4. It is thought to represent the primordial distribution of separations for wide binaries both from theoretical reasons (Valtonen 1997) and from observations (it holds for the youngest binaries up to their largest separations, see (Poveda & Hernández-Alcántara 2003; Poveda et al. 2007).

5. We have shown above that it holds for tha ChG halo binaries. Indeed, we found it holds also for their disk binaries, and explains in a natural way, as the result of dissolution effects, the flattening of their distribution, which ChG found puzzling, and for which they offered no explanation.

The cumulative frequency distribution of the angular separations for the more halo-like sample of 211 binaries is shown in Figure 8, that of the expected semiaxes in Figure 9. It is clearly seen that they follow Oepik's distribution. We performed KS tests to support this assertion, and found that Oepik's distribution holds up to angular separations of 160 arc seconds, and to expected semiaxes of 25 000 AU (0.12 pc). The latter test is shown in Figure 10.

To further refine our sample of halo candidates we integrated galactic orbits for all binaries with available radial velocities (150), and calculated the times they spend in the galactic disk, that is, between z-distances of ±500 pc. Figures 11, 12 and 13 display the meridional orbits of three representative binaries. The cumulative frequency distribution of expected major semiaxes for this sample is shown in Figure 14, the result of the KS test in Figure 15. The preceding figures clearly show that Oepik's distribution holds for all these subsamples, although it does so up to different values of the separations or major semiaxes.

Next, we separated the 150 binaries into three groups (each with an equal number of binaries), according to the time they spend within the galactic disk, as defined above. We refer to these groups as the most disk-like, the intermediate, and the most halo-like binaries. The average fraction of their lifetime the 50 most disk-like binaries spend in the disk is 100%, that of the most halo-like binaries is 18%. To maximize the contrast we disregarded the intermediate group.

Figures 16 and 17 show the cumulative frequency distribution of the expected major semiaxes for the most disk-like and the most halo-like groups. The corresponding KS tests are displayed in Figures 18 and 19. We see that the most disk-like binaries follow Oepik's distribution up to an expected major semiaxis of 19,000 AU (0.09 pc), while the most halo-like binaries do so up to an expected semiaxis of 63,000 AU (0.31 pc).

These results confirm and reinforce the conclusions obtained in (Poveda et al. 1997; Allen et al. 2000) and (Poveda & Allen 2004), namely that (a) Oepik's distribution is followed by many different samples of wide binaries; (b) that the maximum semiaxis up to which Oepik's distribution holds is a function of the age of the group studied, as well as of the environment encountered by the binary along its galactic trajectory. Thus, for example, (Poveda et al. 1994) were able to divide the binaries in their catalog in two groups, "probably young" (2×10^9 yr) and "probably old" ($> 4.6 \times 10^9$ yr), according to a variety of age indicators. (Poveda & Allen 2004) found Oepik's law to be valid up to semiaxes of 8,000 AU for the young group, and up to only 2400 AU for the old group. For a very young (10^6 yr) independent group of binaries in the Orion Nebula Cluster:

(Poveda & Hernández-Alcántara 2003) found Oepik's distribution to hold up to 45,000 AU.

The departure from Oepik's distribution can be interpreted as due to the effects of dynamical perturbations, which tend to decrease the binding energy and thus increase the separation of the binary, until its ultimate dissolution. These effects, with the passage of time, will tend to eliminate the widest systems. (Weinberg et al. 1987; Wasserman & Weinberg 1991) and more recently (Jiang & Tremaine 2010) have modeled the evolution of disk binaries subject to perturbations by passing stars and molecular clouds. The former authors find galactic tides to have negligible effects for binaries with $a < 0.65$ pc, the latter take tides into consideration for their widest binaries ($a > 10^5$ AU). Our widest binaries would thus appear to be stable against galactic rides. The results of Weinberg et al. were found to be consistent with the distributions found for the youngest and oldest systems of the solar vicinity (Poveda et al. 1997). For the samples studied here, the departure from Oepik's distribution sets in at much larger values than those obtained for even the oldest binaries of the solar vicinity. Similarly as was done in (Allen et al. 2000) we interpret these larger values as due mainly to the relatively small time spent by our binaries within the galactic disk, where most of the perturbations occur. The most halo-like binaries in (Allen et al. 2000) spent on average 26% of their lifetimes within the disk, and were found to follow Oepik's distribution up to $\langle a \rangle = 20,000$ AU (0.1 pc). The most halo-like binaries of our improved catalogue spend on average only 18% of their lifetime within the disk and follow Oepik's distribution up to 63,000 AU (0.31 pc).

The question arises as to the effects of observational uncertainties on our results. Uncertainties in the distances will affect directly the inferred semiaxes, but not their distribution. The galactic orbits will be affected by uncertainties in the distances, proper motions and radial velocities. We have estimated the errors in the orbital parameters listed in Table 1 for a representative sample of binaries. To this end, we computed for each binary two extreme orbits by adding and subtracting all the uncertainties to the "central" values. This will provide an overestimate of the expected errors in the orbital parameters. The average resulting errors for this sample turned out to be 18% for $R_{\max}$, 14% for $z_{\max}$ and 16% for e. Binary membership into the most halo-like and the most disk-like groups remained unchanged.

4. Discussion and conclusions

By means of an extensive literature search we have compiled a list of 251 candidate halo wide binaries and present it in Table 1. Proper motions, radial velocities, photometric data and distances were carefully checked for each system. We found that the distribution of separations and major semiaxes for all the subgroups studied follows Oepik's up to different limiting semiaxes. We computed galactic orbits for 150 binaries and obtained the fraction of their lifetimes spent within

the galactic disk. Separating the binaries into three groups, most disk.like, intermediate and most halo-like we find that the most disk-like binaries begin to depart from Oepik's distribution at an $\langle a \rangle = 19,000$ AU, whereas the most halo-like do so at an $\langle a \rangle = 63,000$ AU.

The great majority of the wide binaries in our catalog stem ultimately from Luyten's NLTT. The NLTT is quite complete up to visual magnitude 19, and for proper motions larger than 180 mas/yr. As such, it is a magnitude limited sample, and subject to the usual biases of such samples, namely, Malmquist, kinematical, and Lutz-Kelker biases. The rNLTT (Gould & Salim 2003; Salim & Gould 2003) covers the intersection of the First Palomar Observatory Sky Survey and the Second Incremental Release of the Two Micron Sky Survey, about 45% of the sky. As discussed by ChG, it is not necessary to have a volume-complete catalog, but a representative sample, with well understood selection effects. Our catalog, as well as previous ones, is far from complete. Certainly, many of the widest pairs will be missing. However, our main results on the distribution of semiaxes (showing the destructive effects of perturbers at large semiaxes), are not likely to be affected by incompleteness or biases. Oepik's distribution was previously found to hold for a volume-complete sample of nearby wide binaries (Poveda & Allen 2004; Poveda et al. 2007) in the interval 133 AU $< \langle a \rangle <$ 1640 AU. The same distribution was also found to hold (up to different values of the semiaxis) for different, independent samples of binaries, stemming from the LDS, the IDS amd the catalog of nearby wide binaries of (Poveda et al. 1994). Using a variety of age indicators, the latter binaries were separated into young and old groups; the limiting $\langle a \rangle$ turned out to be 2400 AU for the oldest group and 7900 AU for the youngest group. Oepik's distribution was also found to hold up to $\langle a \rangle = 30\,000$ AU for a group of extremely young (10^6 yr) wide binaries in the Orion Nebula Cluster (Poveda & Hernández-Alcántara 2003). It was also shown to hold for the disk and halo binaries of ChG (Poveda et al. 2007). We should mention that the Oepik distribution of separations was also found by (Lépine & Bongiorno 2007) and (Sesar et al. 2008) in their catalogs. The consistency found between our present results and those previously found for many different and independent samples of binaries gives us confidence that incompleteness and selection effects are not significantly influencing our conclusions.

The origin of wide binaries has been a long-standing problem. Several mechanisms have been proposed for this problem, among which we can mention the dynamical unfolding of triple systems (Reipurth & Mikkola 2012), formation by capture of unbound stars in dissolving star clusters (Kouwenhoven et al. 2010; Moeckel & Clarke 2011; Perets & Kouwenhoven 2012), and the suggestion that they may be the sole remains of former moving groups or accreted structures in the galactic halo (Allen & Poveda 2007). Some of these scenarios have as a result a thermal distribution of eccentricities, and an Oepik-like distribution of semiaxes, and would thus accord better with the empirical findings on the distribution of separations of binaries found in different environments and having different ages. It is not clear which of these mechanisms -if any- would work for the halo binaries, but at this stage the scenarios involving cluster dissolution would seem

more plausible, since they result in a thermal distribution of eccentricities and-in some cases- an Oepik-like distribution of semiaxes.

Our present results are consistent with those found in (Allen et al. 2000) with a smaller sample. In a companion paper we show that they allow us to obtain better estimates of the masses of the halo perturbers, and they should be also useful for other dynamical studies.

Acknowledgments. We thank A. Poveda, whose long-time interest in wide binaries inspired this work. MAM is grateful to UNAM-CEP for a graduate fellowship. Our thanks are also due to M. Hernández-Cruz for valuable assistance. This research used the Simbad database operated at CDS, Strasbourg, France.

REFERENCES

Alcock,C. Allsman,R.A. Alves,D. et al. 1998, ApJ, 499, L9

Alcock, C., Allsman, R. A., Alves, D. R. et al. 2001, ApJ, 550, L169

Allen,C. & Santillán, A. 1991, RMxAA 22, 255

Allen, C., Poveda, A. & Herrera, M. A. 1997, in Visual Double Stars : Formation, Dynamics and Evolutionary Tracks. J.A. Docobo, A. Elipe, and H. McAlister. Dordrecht: Kluwer Academic, ASSL. 223, p. 133

Allen, C., Poveda, A. & Herrera, M.A. 2000, A&A, 356, 529

Allen, C. & Poveda, A. 2007, in Binary Stars as Critical Tools & Tests in Contemporary Astrophysics, IAU Symposium 240, Eds. W.I. Hartkopf, E.F. Guinan and P. Harmanec. Cambridge: Cambridge University Press, p. 405

Allen, C. & Monroy-Rodríguez, M.A. 2013, ApJ, submitted

Afonso, C., Albert, J. N., Andersen, J. et al. 2003, A&A, 400, 951

Bartkevičius, A. 2008, Baltic Astronomy, 17, 209

Chanamé, J. & Gould, A. 2004, ApJ, 601, 289

Couteau, P. 1960, J. des Observateurs, 43, 41

Duquennoy, A. & Mayor, M. 1991, A&A, 248, 485

Gould, A. & Salim, S. 2003, ApJ, 582, 1001

Hartkopf, W. I., & Mason B. D., 2007, Sixth Catalog of Orbits of Visual Binary Stars, WDS06, U.S. Naval Observatory, Washington

Jiang, Y. & Tremaine, S. 2010, MNRAS, 401, 977

Kouwenhoven, M. B., Goodwin, S. P., Parker, R. J. et al. 2010, MNRAS404, 1835

Lacey, G. C., & Ostriker, J. P. 1985, ApJ, 299, 633

Lépine, S. & Bongiorno, B. 2007, AJ, 133, 889

Luyten, W. J. 1979, New Luyten Catalog of Stars with Proper Motions Larger than Two-Tenths of an Arcsecond (Minneapolis: Univ. MinnesotaPress)

Mason, B. D., Wycoff, G. L., Hartkopf, W.I. 2007, The Washington Double Star Catalog. WDS, U.S. Naval Observatory, Washington

Moeckel, N., & Clarke, C. 2011, MNRAS, 415, 1179

Nissen, P. E. & Schuster, W. J., 1991, A&A, 251, 457

Oepik, E. J., 1924, Tartu Obs., 25,6

Perets, H. & Kouwenhoven, M. B. 2012, ApJ, 750, 83

Poveda, A. & Allen, C. 2004, IAU Colloquium 191 - The Enviroment and Evolution of Double and Multiple Stars, C. Allen & C. Scarfe, RMxAA 21, 49

Poveda, A., Allen, C. & Hernández-Alcántara, A. 2007, in Binary Stars as Critical Tools & Tests in Contemporary Astrophysics, IAU Symposium 240, Eds. W.I. Hartkopf, E.F. Guinan and P. Harmanec. Cambridge: Cambridge University Press, p. 417

Poveda, A., Allen, C. & Herrera, M. A. 1997, Visual Double Stars : Formation, Dynamics and Evolutionary Tracks. J.A. Docobo, A. Elipe, and H. McAlister. Dordrecht : Kluwer Academic, ASSL 223, 191

Poveda, A. & Hernández-Alcántara, A. 2003, Stellar astrophysics. Sixth Pacific Rim Conference. Cheng, K. S., Leung, K. C. and Li. T. P. Dordrecht : Kluwer Academic, ASSL 298,111

Poveda, A.,Herrera, M.A., Allen, C., Cordero, G. & Lavalley, C. 1994, RMxAA 28, 43

Quinn, D. P., Wilkinson, M. I., Irwin, M. J. et al. 2009, MNRAS, 396, 1, L11

Raghavan, D., McAlister, H. A., Henry, T. et al. 2010, ApJS, 190, 1

Reipurth, B. & Mikkola, S. 2012, Nature, 492, 221

Ryan, S. G. 1992, AJ, 104, 1144

Salim, S. & Gould, A. 2003, ApJ, 582, 1011

Sesar, B., Ivezić, Z. & Jurić, M. 2008, AJ, 689, 1244

Valtonen, M. 1997, Visual Double Stars : Formation, Dynamics and Evolutionary Tracks. J.A. Docobo, A. Elipe, and H. McAlister. Dordrecht : Kluwer Academic, ASSL. 223, 241

Wasserman, I. & Weinberg, M. D. 1991, ApJ, 382, 149

Weinberg, M. D., Shapiro S. L. & Wasserman I. 1987, ApJ, 312, 367

Yoo, J., Chanamé, J. & Gould, A. 2004, ApJ, 601, 311

Zapatero-Osorio, M.R. & Martín, E. L. 2004, A&A, 419, 167

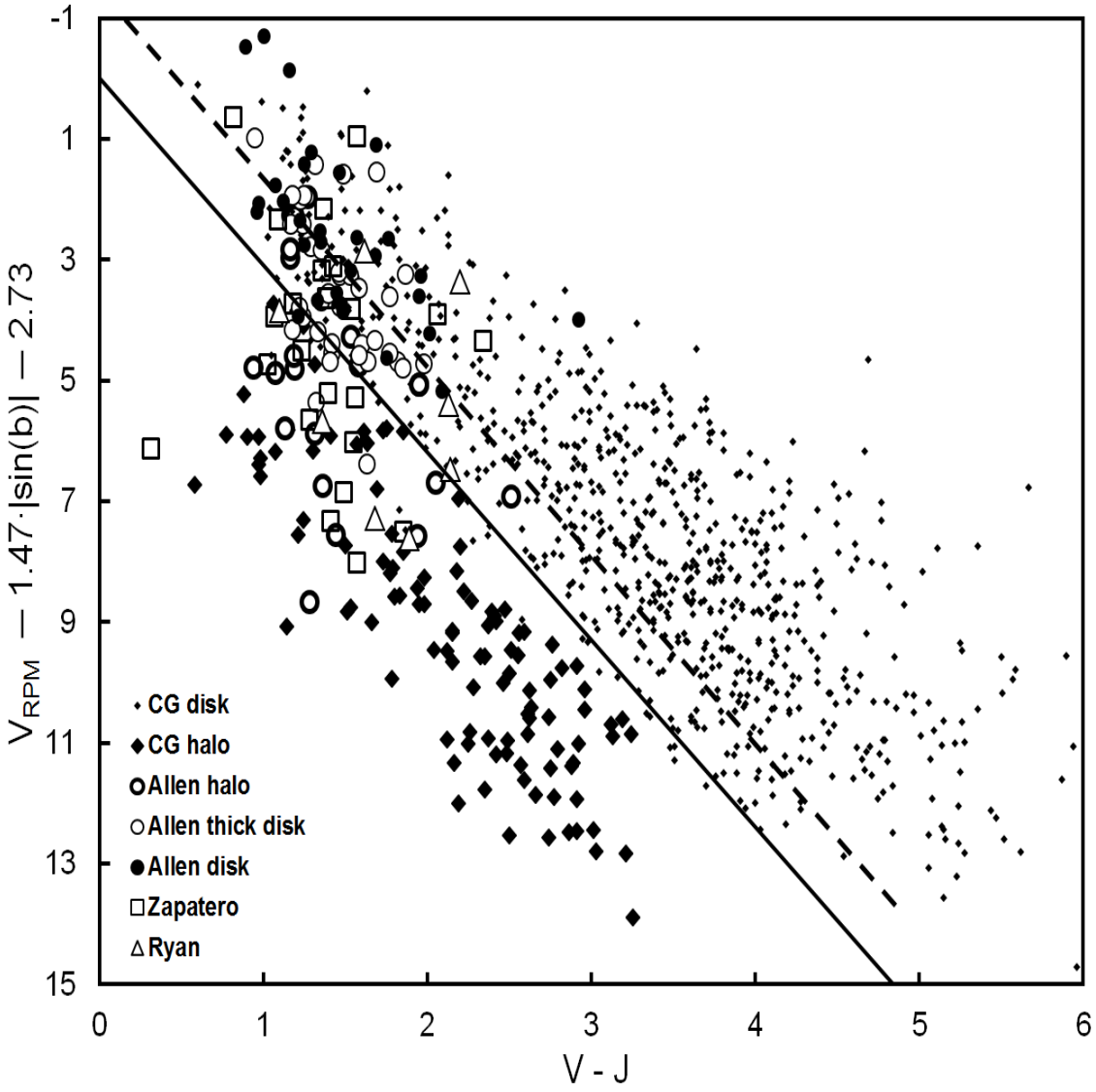

Fig. 1.— Reduced proper motion diagram for 251 halo wide binary candidates. The axes are defined as in ChG (their eq. 2). The V-J plotted is that of the primaries. The vertical axis plots the reduced proper motion adjusted for galactic latitude b. Here $V_{\rm RPM} = V + 5\log\mu$, with V the $V-$magnitude and μ the proper motion. The symbols denote the provenance from different catalogues. The full line was used by ChG to separate disk from halo binaries. However, this line excludes quite a number of binaries whose galactic orbits clearly indicate membership to the halo as was shown in Allen et al. (2000). To identify candidate halo binaries we shifted the ChG line so as to include these stars, as shown by the dashed line. Final halo membership was determined by computing the time the binaries spend within the galactic disk. See text for details

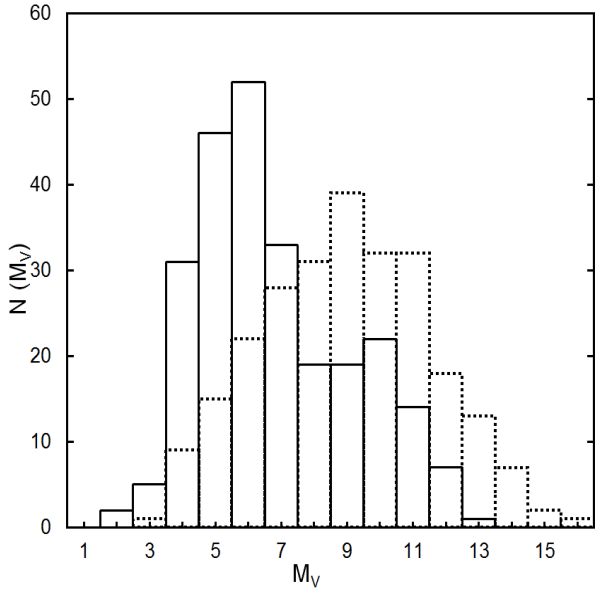

Fig. 2.— Frequency distribution of the absolute magnitudes of 251 halo wide binary candidates. The primaries (full line) and secondaries (dashed line) are shown. Note the extension of the magnitudes of the secondaries to the faint end of the diagram.

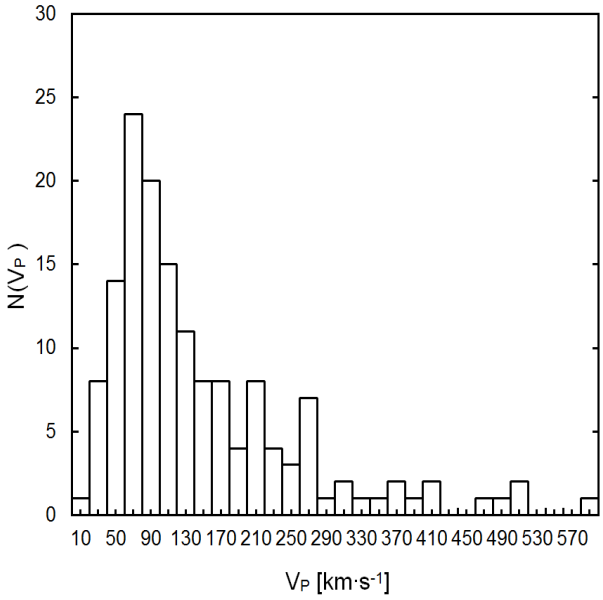

Fig. 3.— Frequency distribution of the peculiar velocities of 150 binaries with available radial velocities. Note that the majority of these stars have peculiar velocities much larger than 65 km s^{-1}, clearly indicating that halo binaries predominate in this sample.

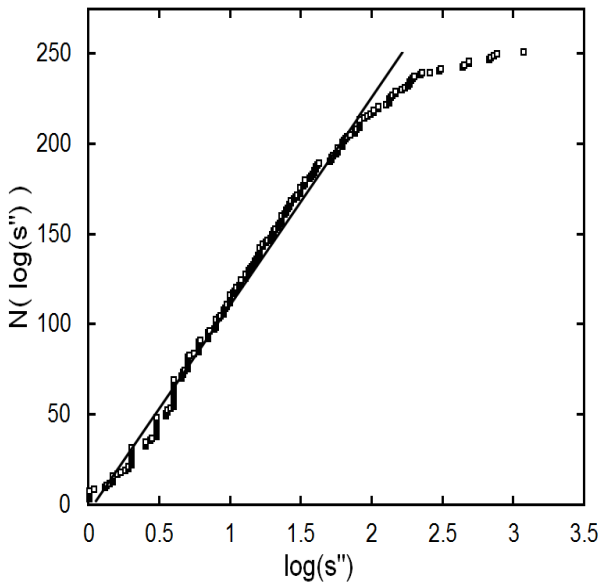

Fig. 4.— Cumulative distribution of the angular separations of 251 halo wide binary candidates. The full line is a fit to the Oepik distribution $f(s)$ = k/s.

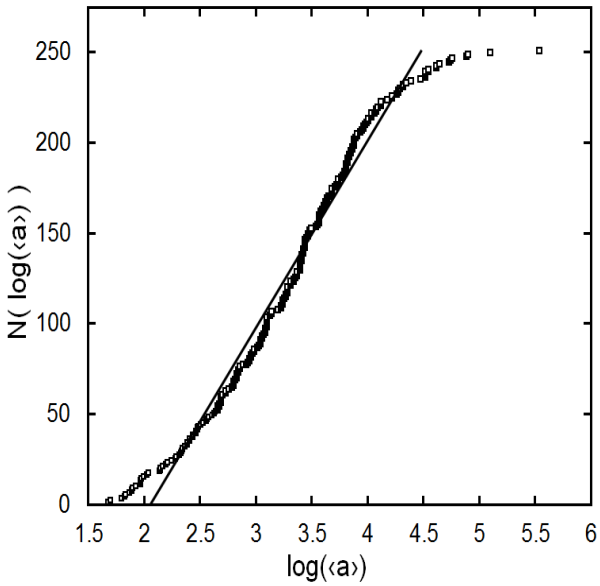

Fig. 5.— Cumulative distribution of the expected major semiaxes of 251 halo wide binary candidates. The full line is a fit to the Oepik distribution $f(\langle a \rangle) = k\langle a \rangle^{-1}$. Units for $\langle a \rangle$ are AU.

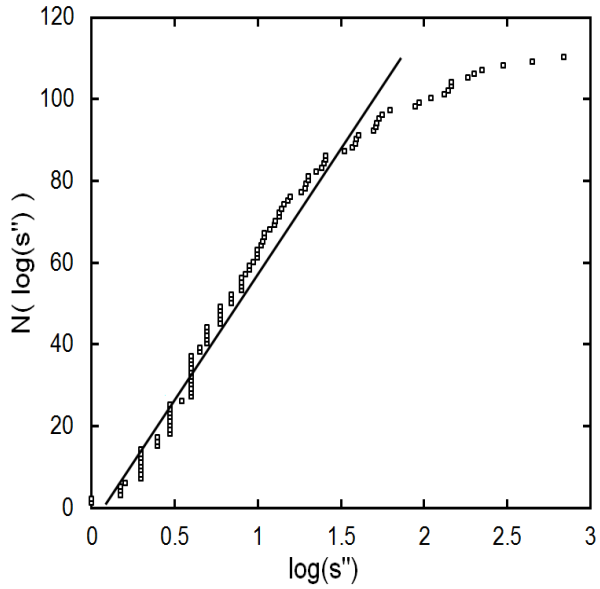

Fig. 6.— Cumulative distribution of the angular separations of the 110 ChG halo wide binaries. The full line is a fit to the Oepik distribution $f(\langle a \rangle) = k\langle a \rangle^{-1}$. The fit is seen to satisfactorily represent this sample.

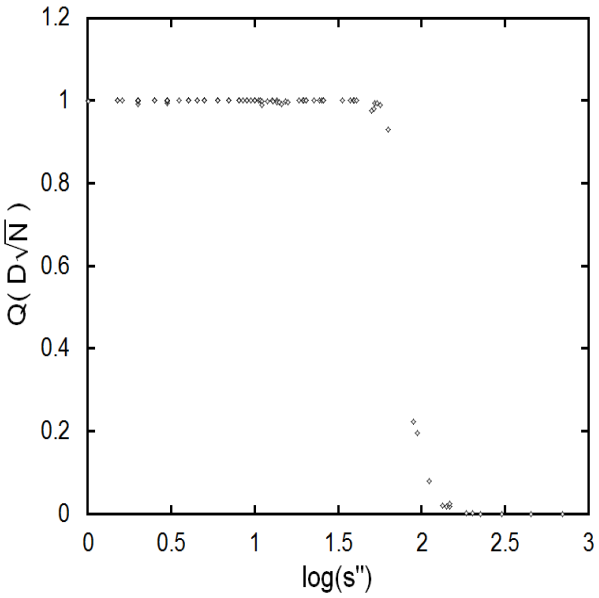

Fig. 7.— Result of applying the Kolmogorov-Smirnov test to the binaries of ChG shown in Figure 6. The coefficient of significance Q is plotted as the ordinate. The test shows that the fit is excellent up to a separation of 63 arc seconds (97 binaries), where it abruptly deviates from the Oepik distribution. See text for details.

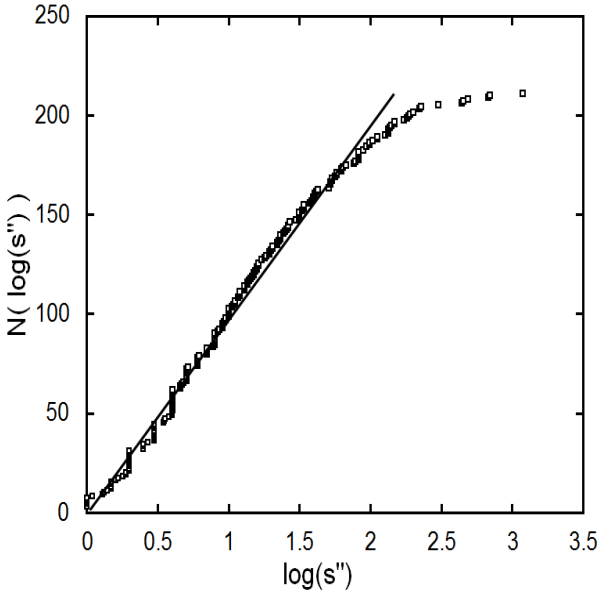

Fig. 8.— Cumulative distribution of the angular separations of the sample of 211 halo wide binary candidates. The full line is a fit to the Oepik distribution $f(s) = k/s$.

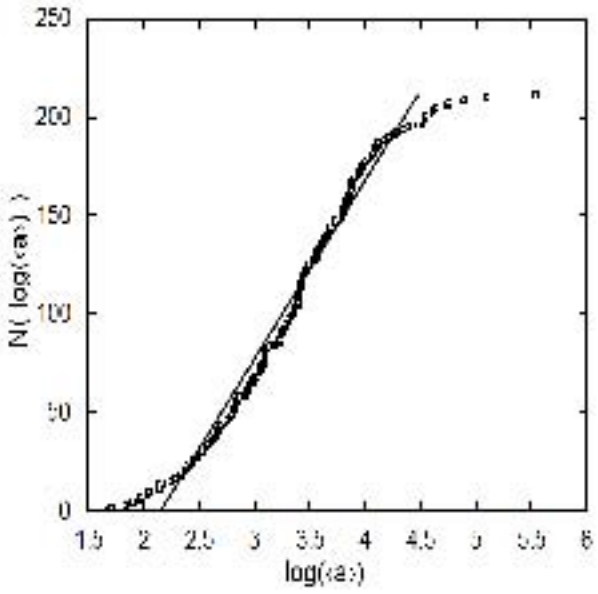

Fig. 9.— Cumulative distribution of the expected major semiaxes of the sample of 211 halo wide binary candidates. The full line is a fit to the Oepik distribution $f(\langle a \rangle) = k\langle a \rangle^{-1}$. Units for $\langle a \rangle$ are AU.

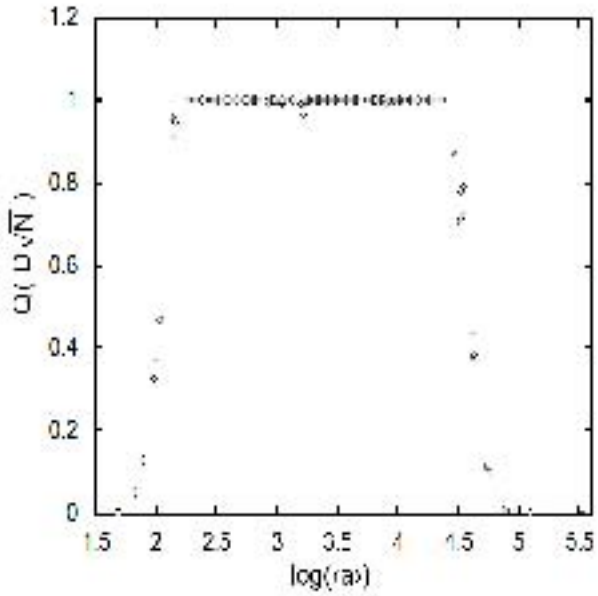

Fig. 10.— Result of the Kolmogorov-Smirnov test for the 211 binaries of Figure 9. Units for $\langle a \rangle$ are AU. The test shows that the Oepik ditribution holds up to an expected major semiaxis of 25 000 AU.

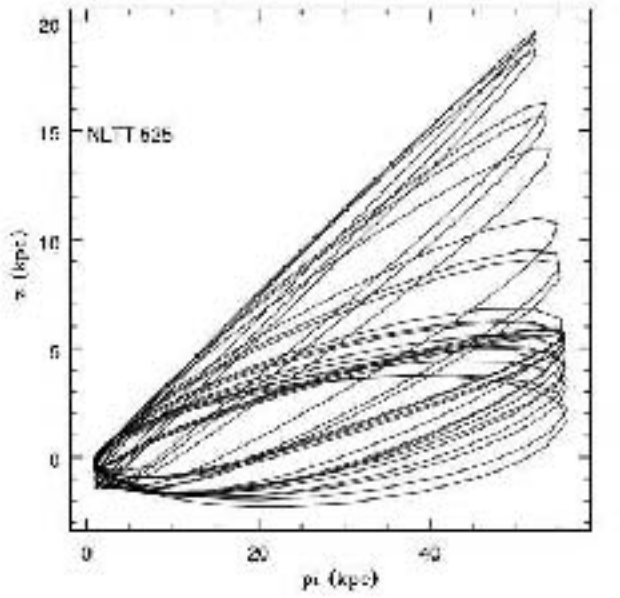

Fig. 11.— Meridional galactic orbit of the binary NLTT 525/526. This binary spends 15.7% of its lifetime within the galactic disk.

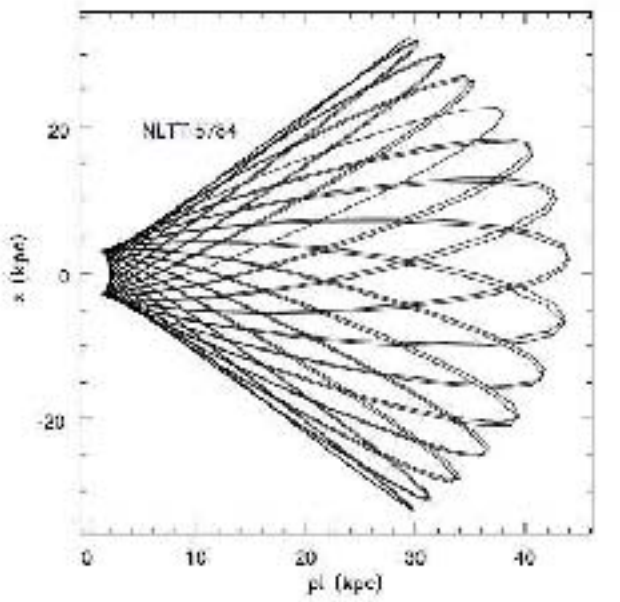

Fig. 12.— Meridional galactic orbit of the binary NLTT 5781/5784. This binary spends 1.9% of its lifetime within the galactic disk.

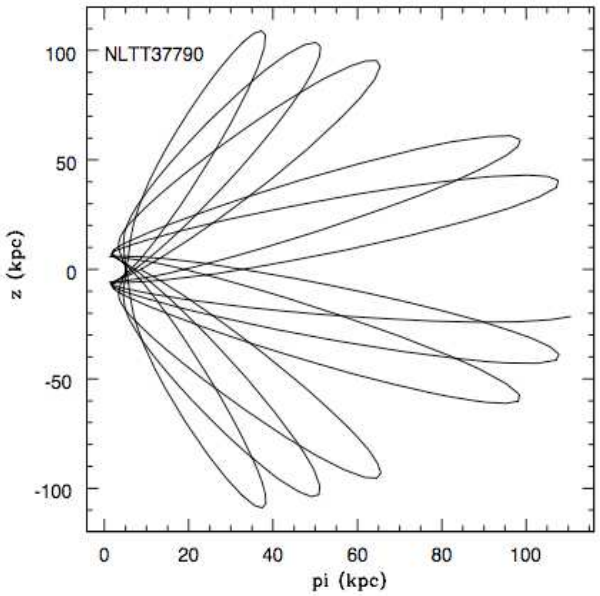

Fig. 13.— Meridional galactic orbit of the binary NLTT 37790/37787. This binary spends 0.3% of its lifetime within the galactic disk.

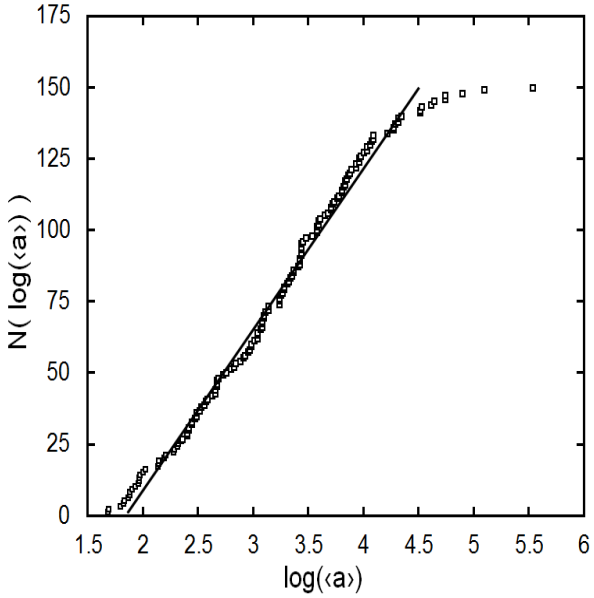

Fig. 14.— Cumulative distribution of the expected major semiaxes of 150 halo wide binary candidates with computed galactic orbits. Units for $\langle a \rangle$ are AU. The full line is a fit to the Oepik distribution $f(\langle a \rangle) = k/(\langle a \rangle)$

.

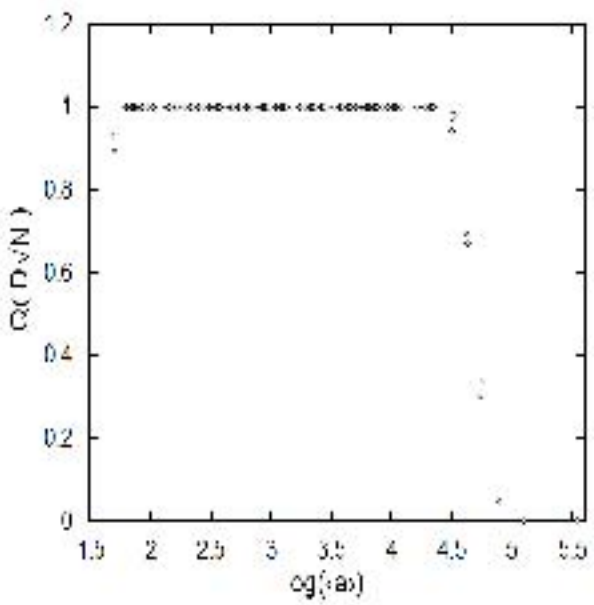

Fig. 15.— Result of applying the Kolmogorov-Smirnov test to the150 binaries of Figure 14. The test shows that the fit is excellent up to an expected major semiaxis of 28,200 AU, and then abruptly deviates from the Oepik distribution. We interpret this departure as due to dynamical effects which tend to dissociate the widest binaries. See text for details.

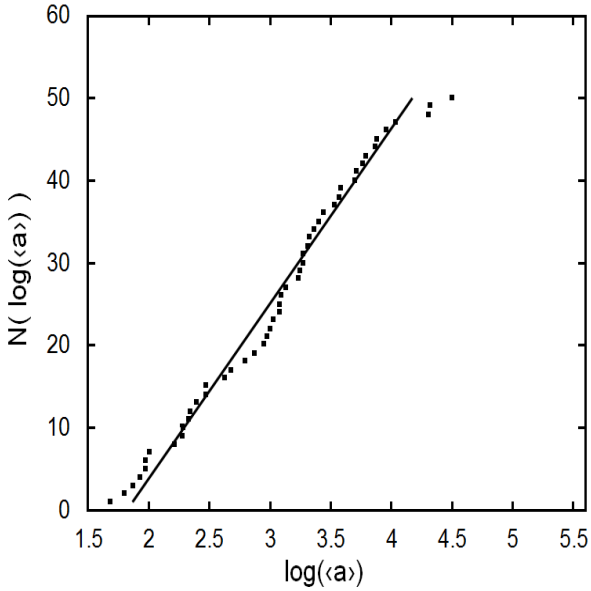

Fig. 16.— Cumulative distribution of the expected major semiaxes of 50 most disk-like wide binaries with computed galactic orbits. These binaries spend just about their entire lifetimes within the galactic disk. Units for $\langle a \rangle$ are AU. The full line is a fit to the Oepik distribution $f(\langle a \rangle) = k/(\langle a \rangle)$

.

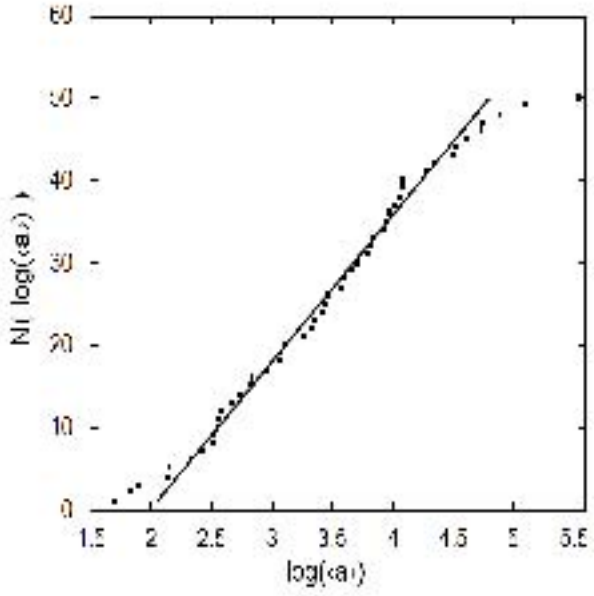

Fig. 17.— Cumulative distribution of the expected major semiaxes of 50 most halo-like wide binaries with computed galactic orbits. These binaries spend an average of 18% of their lifetimes within the galactic disk. Units for $\langle a \rangle$ are AU. The full line is a fit to the Oepik distribution $f(\langle a \rangle) = k/(\langle a \rangle)$.

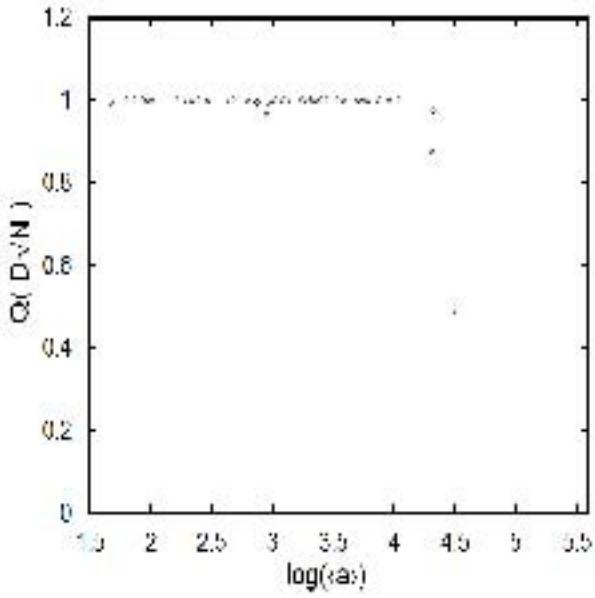

Fig. 18.— Result of applying the Kolmogorov-Smirnov test to the 50 most disk-like binaries of Figure 16. Units for $\langle a \rangle$ are AU. The test shows that the fit is excellent up to an expected major semiaxis of 15 000 AU, and then abruptly deviates from the Oepik distribution.

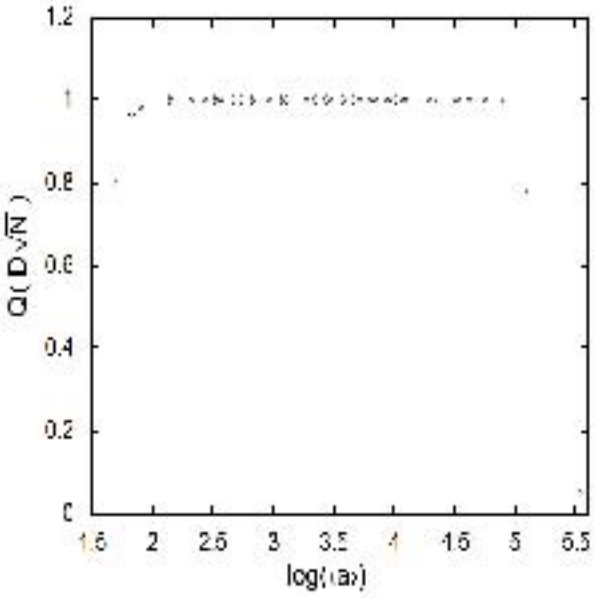

Fig. 19.— Result of applying the Kolmogorov-Smirnov test to the 50 most halo -like binaries of Figure 17. Units for $\langle a \rangle$ are AU. The test shows that the fit is excellent up to an expected major semiaxis of 63 000 AU, and then abruptly deviates from the Oepik distribution. This result shows that Oepik's distribution holds up to much larger values of the semiaxes as the binaries spend shorter fractions of their lifetimes within the galactic disk.

Table 1. Improved Catalog of Candidate Halo Wide Binaries

Primary	Other ID	Secondary	d (pc)	$M_V(p)$	M_V(s)	s (")	$\langle a \rangle$ (AU)	v_p (km/s)	R_{max} (kpc)	$\lvert z_{max} \rvert$ (pc)	e	t_d/t	Cat
(1)	(2)	(3)	(4)	(5)	(6)	(7)	(8)	(9)	(10)	(11)	(12)	(13)	(14)
NLTT 58746		NLTT 58747	156	9.4	9.4	4	876						CG
NLTT 58812		NLTT 58813	435	6.2	6.2	2	1217						CG
NLTT 239		NLTT 240	496	10.0	10.0	10	6944						CG
NLTT 403	HIP 754	LP 348-62	45	4.5	8.8	30	1902	33.4	8.6	258	0.11	1.000	A
NLTT 525	HIP 911	NLTT 526	251	4.8	7.4	8.5	2986	361.3	31.6	3122	0.92	0.157	ACG
NLTT 1036		NLTT 1038	290	10.8	6.0	22.5	9135	213.0	9.8	7363	0.29	0.049	CG
NLTT 1412		NLTT 1416	104	9.5	6.7	51.5	7475						CG
NLTT 1645		NLTT 1647	219	7.5	9.9	20.2	6198						CG
NLTT 1806	HIP 2663	BD -35 170B	36	3.6	6.0	6	304	90.9	9.3	146	0.34	1.000	A
NLTT 1945	G 069-004	G 069-004 Ng	53	4.8	5.6	6.16	455	139.5	8.6	921	0.42	0.463	Z
NLTT 2056	G172-016	G172-016B	119	5.6	11.4	8.3	1383	123.7	9.5	523	0.70	0.969	Z
NLTT 2144		NLTT 2145	218	6.5	6.5	4	1220						CG
NLTT 2205		NLTT 2206	170	6.8	8.2	3	713						CG
NLTT 2324		NLTT 2325	198	8.5	8.5	2.5	694						CG
NLTT 2425		NLTT 2426	282	11.3	8.7	4	1580						CG
NLTT 2484	HIP 3550	LP 466-33	63	5.8	13.4	62	5467	69.8	9.7	350	0.22	1.000	A
NLTT 2963		NLTT 2964	397	10.7	11.3	2	1112						CG
NLTT 2989		NLTT 2990	107	9.9	9.9	1	149						CG
NLTT 3116	G 242-074 A	G 242-074 Bn	98	4.8	9.9	19.5	3182	124.5	8.6	1336	0.52	0.284	Z
NLTT 3252		NLTT 3253	503	9.5	10.7	10.8	7607						CG
	HIP 5140	LDS 34	82	4.4	7.8	23	2640	53.5	8.6	528	0.16	0.932	A
NLTT 3847		NLTT 3849	101	8.4	10.9	8	1127						CG
NLTT 4362	HIP 6130	BD -1 167B	28	5.8	9.7	28	1084	49.7	8.6	112	0.21	1.000	A
NLTT 4625		NLTT 4626	802	6.6	4.4	4	4492						CG
NLTT 4814	G 002-038	NLTT 4817	153	10.7	5.2	24.4	5139	303.0	12.9	8058	0.98	0.006	ACG
NLTT 5690	HIP 7869	LP 88-69	71	4.1	9.1	22	2198	183.7	8.6	4562	0.51	0.083	A
NLTT 5781		NLTT 5784	306	11.6	7.1	52.1	22320	380.4	44.2	32637	0.91	0.019	CG
NLTT 6529	HIP 9094	LP 709-81	34	3.8	9.3	29	1379	80.5	12.4	201	0.26	1.000	A
NLTT 7087	HIP 9971	BD 27 335B	57	6.2	6.8	22	1755	86.5	8.6	679	0.32	0.709	A
NLTT 7795	G4-16	LP 579-18	134	7.4	12.3	41	7689	147.8	8.6	468	0.67	1.000	A
NLTT 7845	HIP 11137	BD 14 387	57	5.1	5.6	34	2727	65.4	12.6	657	0.22	0.730	A
NLTT 8447	HIP 12114	BD 6 389B	7	6.5	12.4	170	1715	78.5	11.6	736	0.22	0.580	A
NLTT 8643	HIP 12411	LP 941-143	40	5.3	13.4	31	1738	81.1	8.9	311	0.32	1.000	A
NLTT 8720		NLTT 8721	205	7.2	7.2	6	1719						CG
NLTT 8753		NLTT 8759	206	9.8	10.9	146.3	42122						CG
NLTT 8997	HIP 13081	LP 354-414	22	5.8	13.8	20	626	17.7	8.6	68	0.07	1.000	A
NLTT 9360		NLTT 9361	216	10.3	10.1	18.3	5534						CG
NLTT 9798	HIP 14342	LP 470-9	100	3.6	7.6	1	140	104.5	8.7	2366	0.10	0.121	A
NLTT 9961		NLTT 9962	122	8.7	8.7	4	681						CG
NLTT 10356	HIP 15126	BD 0 549	79	5.7	11.3	78	8686	155.1	12.7	785	0.48	0.644	A
NLTT 10426	HIP 15253	BD 4 519	78	4.8	7.3	2	218	117.8	9.9	76	0.43	1.000	A
NLTT 10597	HIP 15371	BD -63 217	12	4.8	5.2	310	5241	74.0	9.5	321	0.24	1.000	A
NLTT 10514	HIP 15394	BD 14 550B	57	3.6	10.7	135	10772	72.4	8.8	673	0.23	0.669	A
NLTT 10536	HIP 15396	NLTT 10548	214	4.6	9.1	185.7	55410	417.5	9.6	5202	0.12	0.062	ACG

Table 1—Continued

Primary	Other ID	Secondary	d (pc)	$M_V(p)$	M_V(s)	s (")	$\langle a \rangle$ (AU)	v_p (km/s)	R_{max} (kpc)	$\lvert z_{max} \rvert$ (pc)	e	t_d/t	Cat
(1)	(2)	(3)	(4)	(5)	(6)	(7)	(8)	(9)	(10)	(11)	(12)	(13)	(14)
NLTT 10634	HIP 15572	BD 8 496	51	4.9	11.5	81	5752	60.5	8.7	444	0.21	1.000	A
NLTT 10701	HIP 15683	LP 412-34	73	6.6	13.2	26	2656	92.7	9.3	593	0.32	0.844	A
NLTT 10733	HD 20835	LP 155-70	79	4.3	10.5	10	1106	87.2	12.7	817	0.26	0.541	A
NLTT 10780		NLTT 10781	481	8.7	8.7	3	2020						CG
NLTT 10999		NLTT 11000	678	8.4	7.6	14	13288						CG
NLTT 11015		NLTT 11016	152	10.0	11.1	9	1920						CG
NLTT 11139		NLTT 11140	113	6.7	6.5	4	631						CG
NLTT 11124	HIP 16467	BD 43 744B	54	4.9	9.4	16	1205	70.2	8.9	318	0.27	1.000	A
NLTT 11330	L 91-93	L91-94	34	8.4	8.8	13	448						R
NLTT 11288		NLTT 11300	176	8.4	5.2	223.5	55082						CG
NLTT 11424	G6-22	LP 413-23	108	6.1	6.3	3	453	143.6	10.5	891	0.48	0.528	A
NLTT 11538		NLTT 11539	366	4.0	4.0	6	3072						CG
NLTT 11791	HIP 17666	NLTT 11792	25	6.9	6.3	8	274	151.4	9.6	1603	0.51	0.242	ACG
NLTT 12294		NLTT 12296	189	11.9	8.7	40.5	10691						CG
NLTT 12415	HIP 18824	LP 944-99	52	3.1	3.7	1.9	139	86.9	8.7	1094	0.25	0.341	A
NLTT 12415	HIP 18824		52	3.1	14.9	64	4678	86.9	8.7	1094	0.25	0.341	A
NLTT 12567	HIP 19255		21	5.6	3.8	720	20739	24.2	9.0	27	0.08	1.000	A
NLTT 12567	HIP 19255	BD 37 878B	21	5.6	7.4	3.6	74	24.2	9.0	27	0.08	1.000	A
NLTT 12863	HIP 19849	BD -7 781A	5	5.9	10.8	82	578	111.2	12.7	624	0.34	0.815	A
	Lp 230-119	Lp 230-125	84	8.5	8.5	31	2606						R
NLTT 13455	HD 283702	BD 26 727B	80	6.4	8.5	16	1791	92.1	8.6	144	0.41	1.000	A
NLTT 13968		NLTT 13970	148	5.7	12.9	20.3	4209						CG
NLTT 14005	G85-17	NLTT 13996	103	5.7	12.6	133	19173	101.9	8.7	2000	0.20	0.157	A
NLTT 14142	HD 31208	BD 7 754B	34	5.5	5.8	16	761	53.0	8.7	41	0.22	1.000	A
NLTT 14407		NLTT 14408	47	8.5	11.2	11	725						CG
NLTT 14658		NLTT 14659	174	5.8	5.8	2.5	609						CG
NLTT 14867	HIP 24819	BD -3 1061B	17	6.6	6.6	4	94	90.6	9.7	363	0.31	1.000	A
NLTT 14943	HIP 25137	LP 638-4	62	5.3	9.1	76	6591	80.6	12.4	1196	0.22	0.307	A
NLTT 15008		NLTT 15009	144	10.4	12.9	12.7	2554						CG
NLTT 15113	G 99-8	G99-9	114	8.0	9.5	83	9467						R
NLTT 15262	HIP 26018	BD 19 953	46	5.5	7.3	4	258	56.5	8.7	607	0.16	0.766	A
NLTT 15426	HIP 26501	BD -46 1936B	25	5.3	7.9	5.5	194	63.1	10.4	253	0.19	1.000	A
NLTT 15512	HIP 26907	BD 2 1041B	31	6.1	11.2	53	2325	88.9	8.5	130	0.40	1.000	A
NLTT 15501		NLTT 15509	210	10.6	11.0	141	41454	328.6	28.2	1481	0.85	0.374	CG
NLTT 15664		NLTT 15665	45	11.8	11.8	3.5	222						CG
NLTT 15953		NLTT 15954	122	10.4	13.3	14.4	2466						CG
NLTT 15973	HIP 28671	LTT 9457	39	6.4	9.8	7	382	258.6	16.4	1822	0.76	0.220	A
NLTT 16062	HIP 28940	BD 34 567	70	6.6	10.4	12	1176	265.5	11.8	6401	0.94	0.103	A
NLTT 16184		NLTT 16185	457	5.9	7.4	4.5	2879						CG
NLTT 16394		NLTT 16407	348	4.5	7.6	698.5	340309	481.5	144.0	88786	0.90	0.003	CG
NLTT 16629		NLTT 16631	55	6.4	10.5	434.1	33416	179.6	8.9	2562	0.29	0.125	CG
NLTT 16747	HIP 31740	LP 160-41	84	5.5	13.7	62	7280	131.8	9.9	784	0.46	0.619	A
NLTT 16948	HIP 32423	R 419	25	6.8	11.0	31	1084	70.7	13.7	916	0.24	0.458	A
NLTT 17017	HIP 32650	LDS 5686	50	4.4	12.4	27	1893	128.3	12.6	1116	0.37	0.376	A

Table 1—Continued

Primary	Other ID	Secondary	d (pc)	$M_V(p)$	M_V(s)	s (")	$\langle a \rangle$ (AU)	v_p (km/s)	R_{max} (kpc)	$\lvert z_{max} \rvert$ (pc)	e	t_d/t	Cat
(1)	(2)	(3)	(4)	(5)	(6)	(7)	(8)	(9)	(10)	(11)	(12)	(13)	(14)
NLTT 17116	G 192-57	LP122-11	238	5.4	8.3	103	24538						R
NLTT 17382	HIP 34065	BD -43 2907	16	4.5	5.6	21	478	75.7	8.8	156	0.30	1.000	A
NLTT 17382	HIP 34065	BD -43 2904	16	4.5	8.1	193	4389	75.7	8.8	156	0.30	1.000	A
NLTT 17675	HIP 35599	LP 58-160	85	4.3	11.9	58	6868	117.9	10.0	175	0.42	1.000	A
NLTT 17770	HIP 35756	LP 359-227	180	4.1	10.4	34	8565	262.7	11.7	8661	0.96	0.158	A
NLTT 17890	HIP 36165	BD -34 3610	40	4.0	4.6	17	944	76.5	9.4	686	0.22	0.635	A
NLTT 17907	HIP 36357		18	2.9	10.6	2.8	69	39.6	10.9	259	0.14	1.000	A
NLTT 17907	HIP 36357	BD+32 1562	18	6.5	2.9	757	18594	39.6	10.9	259	0.14	1.000	A
NLTT 18247		NLTT 18248	110	6.6	6.2	2	307						CG
NLTT 18346	HIP 37671	NLTT 18347	167	5.1	4.3	11.9	2805	290.3	21.6	17469	0.52	0.028	ACG
NLTT 18775	G 90-036	G090-036B	293	5.4	8.8	1.67	685	515.8	429.1	53116	0.96	0.020	Z
NLTT 18798		NLTT 18799	154	8.9	4.9	12.9	2788						CG
NLTT 19053		NLTT 19054	460	4.3	4.3	4	2578						CG
NLTT 18924		NLTT 18931	79	10.3	5.5	110.4	12210	155.0	9.0	1958	0.44	0.185	CG
NLTT 19210	G 40-14	BD 30 4982B	235	4.5	10.8	98	32233	413.2	16.4	1444	0.70	0.327	A
NLTT 19979		NLTT 19980	344	7.9	10.2	19.6	9439	228.1	15.0	8120	0.92	0.135	CG
NLTT 20201		NLTT 20202	248	11.4	8.1	33.4	11581						CG
NLTT 20699		NLTT 20700	136	9.7	6.8	5	950						CG
NLTT 20892		NLTT 20894	270	9.2	8.0	8	3023						CG
NLTT 20979	G 09-047	G009-047B	89	2.9	11.6	81.93	10217	162.8	10.1	1617	0.62	0.233	Z
NLTT 21061	G116-009	G116-009B	265	7.2	11.2	10.08	3744	105.7	9.6	5395	0.89	0.237	Z
NLTT 21351		NLTT 21352	699	3.6	3.6	2.5	2445						CG
NLTT 21914		NLTT 21915	420	10.1	9.2	8	4703						CG
NLTT 21999	HIP 46853		14	2.5	12.9	5	94	56.2	9.3	220	0.18	1.000	A
NLTT 22230	HIP 47225		34	4.3	9.4	4	191	49.9	8.6	437	0.16	1.000	A
NLTT 22301		NLTT 22302	378	9.3	7.8	13.6	7187						CG
NLTT 22525		NLTT 22526	416	6.2	4.5	5	2908						CG
NLTT 22726	G 43-7	LP 548-41	120	6.3	13.0	15	2519	178.4	13.9	340	0.56	1.000	A
NLTT 23500	HIP 49668	AB	38	4.4	8.1	4.7	248	55.5	8.7	620	0.15	0.705	A
NLTT 23895	BD+23 2207A	BD+23 2207Bv	23	4.0	9.6	7.72	245	206.9	9.3	150	0.16	1.000	Z
NLTT 23937		NLTT 23938	289	9.7	9.7	1	405						CG
NLTT 24638		NLTT 24639	441	5.9	9.9	6	3700						CG
NLTT 25233		NLTT 25234	183	9.8	6.3	9	2300						CG
NLTT 25403		NLTT 25404	177	6.8	5.2	25.9	6415						CG
NLTT 25582	HIP 53165		55	4.4	6.1	1	77	73.3	9.7	403	0.23	1.000	A
NLTT 25623		NLTT 25624	247	8.4	8.4	3	1038						CG
NLTT 26709		NLTT 26710	85	12.0	12.0	1.5	178						CG
NLTT 27069	G 45-48	BD 6 2436B	92	5.4	8.9	18	2318	103.7	14.5	602	0.33	0.853	A
NLTT 27182		NLTT 27188	128	9.4	7.8	39.1	7030						CG
NLTT 28236	G176-046	G176-046D	127	7.1	12.0	4.8	853	100.3	8.7	989	0.63	0.517	Z
NLTT 28289		NLTT 28290	120	10.3	11.1	10	1686						CG
NLTT 28512	HIP 57443	VB 5	9	5.1	15.7	23	297	58.4	9.4	139	0.20	1.000	A
NLTT 29142	HIP 58401	LP 158-35	32	6.4	13.4	23	1027	189.1	8.5	24	0.88	1.000	A
NLTT 29424		NLTT 29425	481	9.3	9.3	3	2020						CG

Table 1—Continued

Primary	Other ID	Secondary	d (pc)	$M_V(p)$	M_V(s)	s (")	$\langle a \rangle$ (AU)	v_p (km/s)	R_{max} (kpc)	$\lvert z_{max} \rvert$ (pc)	e	t_d/t	Cat
(1)	(2)	(3)	(4)	(5)	(6)	(7)	(8)	(9)	(10)	(11)	(12)	(13)	(14)
NLTT 29556	HIP 58962	BD 19 1185B	135	4.7	7.8	1.8	340	266.9	9.5	5962	0.93	0.232	A
NLTT 29553	HIP 58962	NLTT 29556	135	7.8	4.5	11	2267	266.9	9.5	5962	0.93	0.232	ACG
NLTT 29665	HIP 59126	LP 494-38	42	6.5	15.0	66	3836	71.5	8.9	206	0.28	1.000	A
NLTT 29742	HIP 59233	LP 376-84	56	5.8	10.3	16	1254	91.6	10.5	329	0.29	1.000	A
NLTT 29798		NLTT 29799	240	7.7	7.7	2	672						CG
NLTT 29860		NLTT 29862	371	5.0	5.0	7	3635						CG
NLTT 29957	HIP 59532	LPM 416AB	34	4.8	10.3	2	95	113.3	13.2	743	0.34	0.662	A
NLTT 30746		NLTT 30750	169	10.4	10.8	19.4	4593						CG
NLTT 30792		NLTT 30795	370	10.5	7.8	146.7	75889						CG
NLTT 30837		NLTT 30838	340	11.4	4.9	15.7	7473						CG
NLTT 31465	G 59-032	G059-032B	48	5.5		112.03	7535	211.1	10.6	325	0.32	1.000	Z
NLTT 31648	HIP 62041	LP 377-97	75	6.5	13.7	12	1260	68.6	8.6	375	0.28	1.000	A
NLTT 31891		NLTT 31892	227	7.4	7.4	4	1271						CG
NLTT 31917		NLTT 31918	208	8.9	8.9	3	873						CG
NLTT 32187	HIP 62882	VBS 2	80	3.8	7.8	1.9	213	356.1	22.0	9995	0.94	0.055	A
NLTT 32423	HIP 63239	LP 436-66	73	5.5	4.7	58	5934	84.5	11.6	320	0.26	1.000	A
NLTT 33175	HIP 64345	LDS 3735	61	4.8	9.1	82	7015	164.4	14.6	1898	0.47	0.217	A
NLTT 33209	HIP 64386	LDS 947	70	5.6	7.1	446	43652	117.5	11.0	511	0.37	0.980	A
NLTT 33282		NLTT 33283	188	8.7	9.2	10	2635						CG
NLTT 33527	HIP 64797	BD 17 2611B	11	6.3	10.1	4	63	48.8	11.1	50	0.17	1.000	A
NLTT 34609	G255-038 A	G 255-038 Bq	45	6.6	10.3	14.34	901	183.1	9.3	327	0.29	1.000	Z
NLTT 35210	HIP 67246	LDS 3101	31	3.9	7.5	486	20828	68.0	9.1	195	0.25	1.000	A
NLTT 35299	HIP 67408	BD -35 9019B	28	4.3	8.2	12	475	59.8	8.8	33	0.24	1.000	A
NLTT 35953		NLTT 35954	452	10.6	9.8	10.5	6641						CG
NLTT 35991		NLTT 36000	52	11.7	9.1	133.4	9792						CG
NLTT 36418	HIP 69220	BD -44 9130	49	4.9	11.0	4	273	79.8	9.0	795	0.24	0.511	A
NLTT 36418	HIP 69220	BD 44 9130	49	4.9	7.0	57	3893	79.8	9.0	795	0.24	0.511	A
NLTT 36674		NLTT 36675	174	9.4	9.4	2	487						CG
NLTT 37675		NLTT 37676	162	9.3	9.3	2	454						CG
NLTT 37787		NLTT 37790	193	9.9	6.4	200.9	54283	470.0	115.2	109015	0.92	0.003	CG
NLTT 37935	HIP 71505	LP 500-101	99	4.6	5.7	27	3741	140.5	11.3	158	0.46	1.000	A
NLTT 37997	HIP 71735	LDS 485	27	5.2	9.0	490	18825	74.1	11.1	922	0.19	0.422	A
NLTT 38115		NLTT 38116	427	3.9	3.9	6	3583						CG
NLTT 38195	G 66-022	BD +06 2932 B	73	6.1	9.0	3.6	443	267.6	18.1	10301	0.96	0.137	Z
NLTT 39117		NLTT 39119	375	11.1	5.7	56.7	29736						CG
NLTT 39442	HIP 74199	LP 424-27	132	6.4	6.6	677	125073	306.7	15.6	7088	0.87	0.075	A
NLTT 39456	HIP 74235	NLTT 39457	29	6.7	7.1	300.7	12380	592.2	67.0	6410	0.86	0.088	ACG
NLTT 39616	HIP 74549	BD -40 9410	51	4.9	5.0	17	1213	81.6	9.4	216	0.28	1.000	A
NLTT 39941	HIP 75069	Ross 1050	45	6.0	9.3	190	11856	58.9	9.5	656	0.14	0.638	A
NLTT 40737		NLTT 40738	540	8.9	8.9	1.6	1209						CG
NLTT 40901		NLTT 40902	90	10.0	12.0	4	501						CG
NLTT 41756	G 16-25	VB 6	256	6.3	8.7	1.5	537	515.9	19.9	6958	0.43	0.060	A
NLTT 42554		NLTT 42555	262	7.7	10.2	5	1832						CG
NLTT 42846	HIP 80630		66	5.5	11.0	23	2125	186.8	10.8	313	0.67	1.000	A

Table 1—Continued

Primary	Other ID	Secondary	d (pc)	$M_V(p)$	M_V(s)	s (")	$\langle a \rangle$ (AU)	v_p (km/s)	R_{max} (kpc)	$\lvert z_{max} \rvert$ (pc)	e	t_d/t	Cat
(1)	(2)	(3)	(4)	(5)	(6)	(7)	(8)	(9)	(10)	(11)	(12)	(13)	(14)
NLTT 42969	LP745-22	LP745-23	31	9.1	9.6	126	3905						R
NLTT 43097	G153-067	G 017-027j	48	6.2	10.5	1170.7	79139	162.7	9.4	5692	0.69	0.074	Z
NLTT 43594		NLTT 43595	158	6.6	8.0	6	1331						CG
NLTT 44127	HIP 83591	BD -4 4226	11	7.5	9.4	184	2770	74.8	8.9	300	0.28	1.000	A
NLTT 44256		NLTT 44257	139	11.2	11.2	1.5	292						CG
NLTT 44816	HIP 85378	NLTT 44814	69	4.3	5.5	67	6463	128.9	9.0	1489	0.43	0.253	A
NLTT 45000		NLTT 45001	332	11.4	11.1	9.5	4408						CG
NLTT 45605	HIP 87533		66	3.5	7.0	1	93	133.3	9.2	526	0.51	0.955	A
NLTT 45995	HIP 88937		40	4.6	10.1	4.6	260	56.5	8.5	210	0.23	1.000	A
NLTT 46029	HIP 89000		47	2.3	8.3	7.2	473	36.2	8.5	223	0.13	1.000	A
NLTT 46029	HIP 89000		47	2.3	6.6	104	6808	36.2	8.5	223	0.13	1.000	A
NLTT 46118	G204-049	G204-049B	86	6.2	10.5	2.7	324	218.3	12.0	1163	0.50	0.377	Z
NLTT 46748	HIP 91360	LP 690-95	37	5.5	11.9	36	1868	76.1	8.5	57	0.35	1.000	A
NLTT 46857	HIP 91605		24	6.8	10.3	9	301	108.2	13.2	484	0.33	1.000	A
NLTT 47194	HIP 92960	LP 691-17	75	5.8	10.6	33	3452	145.6	11.3	311	0.47	1.000	A
NLTT 47748		NLTT 47749	254	9.1	8.5	7	2490						CG
NLTT 47955	HIP 96333	LP 869-10	72	4.7	9.3	40	4031	102.5	8.8	157	0.43	1.000	A
NLTT 47955	HIP 96333		72	4.7	6.7	1.4	141	102.5	8.8	157	0.43	1.000	A
NLTT 47984	HIP 96402		39	4.6	10.8	3	164	64.3	8.7	257	0.25	1.000	A
NLTT 48072		NLTT 48073	44	11.7	11.7	4.5	276						CG
NLTT 48140		NLTT 48142	171	4.1	6.6	25.7	6135						CG
NLTT 48402	HIP 97940	BD 1 4135	47	5.4	5.7	163	10802	57.2	9.1	290	0.19	1.000	A
NLTT 48402	HIP 97940		47	5.4	8.1	76.8	5089	57.2	9.1	290	0.19	1.000	A
NLTT 48652	HIP 98767	BD 29 3872B	16	4.7	13.8	178	3959	64.4	8.5	990	0.11	0.346	A
NLTT 48686	HIP 99029		75	4.9	6.6	2	210	98.4	8.9	316	0.39	1.000	A
NLTT 48832	HIP 99461	LPM 452	6	6.4	12.5	8	68	130.1	11.3	1139	0.38	0.351	A
NLTT 49312	HIP 100970		37	4.0	7.5	3	157	96.0	9.2	425	0.35	1.000	A
NLTT 49486		NLTT 49487	115	9.8	7.0	4	645						CG
NLTT 49474		NLTT 49477	146	5.3	12.4	89.1	18268						CG
NLTT 49562	G 262-021	G 262-022r	281	6.7	7.2	29.54	12155	370.5	40.0	27828	0.98	0.031	ZR
NLTT 49624		NLTT 49625	254	7.8	7.8	1.5	533						CG
NLTT 49746	G 230-047A	G 230-047Bl	78	5.7	10.7	11.63	1159	226.6	10.9	1007	0.27	0.401	Z
NLTT 49819		NLTT 49821	289	7.1	5.9	25.1	10165						CG
NLTT 49903	G 230-049A	G 230-049Bm	57	4.7	4.8	1.33	106	234.9	11.7	276	0.30	1.000	Z
NLTT 50559	HIP 104214	BD 38 4344	4	7.5	8.3	24.6	86	95.0	10.1	13	0.32	1.000	A
NLTT 50761	HIP 104660		56	4.3	6.3	1.3	101	142.3	10.9	476	0.48	1.000	A
NLTT 50824		NLTT 50827	375	7.0	4.9	62.7	32910						CG
NLTT 51353	HIP 106074	Wolf 478	51	7.6	9.1	1.1	80	278.0	8.8	1919	0.80	0.234	A
NLTT 51353	HIP 106074	LDS 518	51	7.6	12.1	0.7	50	278.0	8.8	1919	0.80	0.234	A
NLTT 51459	G26-8	LP 637-61	72	6.4	9.9	9.5	957	104.9	9.9	52	0.37	1.000	A
NLTT 51479	HIP 106335	LP 564-23	49	6.9	8.6	0.7	48	133.1	10.9	97	0.45	1.000	A
NLTT 51479	HIP 106335	BD 31 3025	49	6.9	12.5	132	9119	133.1	10.9	97	0.45	1.000	A
NLTT 51780	G 93-027	G093-027B	136	6.0	8.7	3.52	672	259.8	14.4	2596	0.45	0.149	Z
NLTT 51964	G188-022	G188-022B	130	4.5	11.4	5.08	922	218.1	12.7	1710	0.62	0.240	Z

Table 1—Continued

Primary	Other ID	Secondary	d (pc)	$M_V(p)$	M_V(s)	s (")	$\langle a \rangle$ (AU)	v_p (km/s)	R_{max} (kpc)	$\lvert z_{max} \rvert$ (pc)	e	t_d/t	Cat
(1)	(2)	(3)	(4)	(5)	(6)	(7)	(8)	(9)	(10)	(11)	(12)	(13)	(14)
NLTT 51992		NLTT 51993	1138	8.0	7.6	3	4779						CG
NLTT 52131	G214-001	G214-001B	170	5.9	11.7	5.14	1221	167.1	10.3	1640	0.64	0.237	Z
NLTT 52532		NLTT 52538	249	7.9	11.9	37.3	12994						CG
NLTT 52648		NLTT 52649	954	6.0	6.0	5	6679						CG
NLTT 52786		NLTT 52787	167	5.8	5.3	2	468	162.4	9.7	3623	0.58	0.123	CG
NLTT 52864	G 18-24		119	6.6	11.0	99	16489	201.9	10.4	757	0.76	0.724	A
NLTT 53061		NLTT 53062	39	9.6	9.6	2	110						CG
NLTT 53254		NLTT 53255	106	9.2	9.6	53.8	7980						CG
NLTT 53376		NLTT 53377	270	9.6	11.8	5	1886						CG
NLTT 53617		NLTT 53618	118	10.1	10.1	3	494						CG
NLTT 54517	LP520-70	LP520-71	107	5.5	8.1	229	24591						R
NLTT 54708	LP521-3	LP521-4	151	5.2	7.1	38	5741						R
NLTT 55277		NLTT 55278	396	5.9	8.6	4	2218						CG
NLTT 55287	HIP 113231	BD -8 5980B	35	5.3	13.6	42	2047	81.0	9.8	154	0.28	1.000	A
NLTT 55326	HIP 113280	BD 16 4838B	32	6.7	8.3	5	225	28.4	8.5	250	0.09	1.000	A
NLTT 55719		NLTT 55720	104	12.7	12.7	3	435						CG
NLTT 55912	G 028-040	LP 581-80	124	5.8	8.9	15.81	2467	178.9	10.5	230	0.53	1.000	Z
NLTT 55994		NLTT 55997	234	5.4	10.4	50	16392						CG
NLTT 56357	HIP 114962	BD -36 13940B	39	6.2	13.8	15	819	237.9	12.9	575	0.78	0.964	A
NLTT 56335	HIP 114980	BD -67 2593	27	6.8	6.6	71	2709	82.5	8.5	380	0.35	1.000	A
NLTT 56392	HIP 115012		55	4.2	5.8	1	77	72.4	8.9	155	0.29	1.000	A
NLTT 56856	HIP 115684	LP 346-72	89	4.9	7.2	260	32230	103.4	10.7	334	0.32	1.000	AZ
NLTT 56926	G216-045	G216-045B	143	5.5	14.0	31.45	6305	257.1	14.4	94	0.43	1.000	Z
NLTT 57220	G128-077	G128-077B	209	6.8	9.6	9.18	2692	210.8	12.3	1047	0.59	0.472	Z
NLTT 57259		NLTT 57262	222	12.4	9.6	13.5	4193						CG
NLTT 57309	HIP 116421		32	4.3	11.4	8	362	131.2	9.0	1407	0.46	0.269	A
NLTT 57558		NLTT 57559	223	10.7	12.2	15.3	4772						CG
NLTT 57749		NLTT 57756	23	10.6	11.3	94.3	3034						CG
NLTT 57823		NLTT 57827	433	10.0	8.8	39.5	23942						CG
NLTT 58235	G273-152	G273-152B	80	5.6	11.3	3.84	430	217.2	10.0	323	0.20	1.000	Z
NLTT 58594		NLTT 58595	388	8.9	8.9	7	3804						CG

V. Introducción al trabajo: "The end of the MACHO era revisited: new limits on MACHO masses from halo wide binaries"

V.1. Cotas a la masas de los MACHOs utilizando binarias abiertas del halo galáctico.

Ya en el 2004, Yoo et al. (2004) propusieron una interesante aplicación de las binarias abiertas del halo galáctico para determinar las características de los perturbadores, en particular, la masa máxima de los MACHOs (por sus siglas en inglés: massive compact halo objects). Utilizando 90 binarias abiertas del halo procedentes del catálogo de Chanamé & Gould (2004) intentaron encontrar los efectos destructivos de los MACHOs en la distribución de las separaciones observadas. En este trabajo, fueron capaces de estimar una masa máxima para estos perturbadores de 43 $M_{\odot}$, con lo cual esencialmente quedaría excluida la existencia de MACHOs el halo galáctico, puesto que se han encontrado otros límites derivados de estudios de microlentes de los proyectos EROS y MACHOS (Afonso et al. 2003 , Alcock 1998, 2001) que establecen que los perturbadores deben tener masas menores que 30 $M_{\odot}$.

Sin embargo, en el 2009 Quinn et al. mostraron que la cota obtenida por Yoo et al. (2004) depende críticamente de de las binarias más abiertas de su catálogo. Aunque Quinn et al. (2009) no lo mencionan explícitamente, el resultado también depende de la función de distribución de las separaciones, la cual según Yoo et al. (2004) puede ser representada por una ley de potencias en todo el intervalo de separaciones observadas, desde 3.5" hasta 900", sin que se observe discontinuidad alguna en este intervalo. Quinn et al. (2009) obtuvieron velocidades radiales para las dos componentes de cuatro de las binarias más abiertas del catálogo de Chanamé & Gould (2004), y encontraron valores concordantes para las velocidades de tres de ellas. Con ello, queda prácticamente establecida su naturaleza física. La cuarta binaria resultó ser una binaria óptica, es decir, la asociación casual de dos estrellas de campo, situadas a distintas distancias de nosotros, y no ligadas gravitacionalmente. Si se excluye esta falsa binaria y se suponen distribuciones tipo ley de potencias con exponentes entre -0.8 y -1.6 para las separaciones observadas, Quinn et al. (2009) encuentran que la masa máxima de los MACHOs aumenta hasta $\approx$500 $M_{\odot}$, resultado que es mucho menos restrictivo que el previamente

encontrado. Su conclusión es que la muestra disponible de binarias abiertas del halo es demasiado pequeña como para poder establecer límites confiables a la masa de los MACHOs. Por otra parte, señalan que la densidad del halo no es constante, y por ende, el número de MACHOs que perturban a las binarias en el halo no es constante para distintos radios galactocéntricos, como lo supusieron Yoo et al. (2004), y hacen notar que esta variación a lo largo de las órbitas galácticas de las binarias debe ser tomada en cuenta.

V.2. Un mejor cálculo de la cota superior a la masa de los MACHOs.

Utilizamos las binarias de nuestro catálogo con objeto de obtener nuevos límites a las masas de los MACHOs, más confiables, por el uso de un catálogo de estrellas binarias más completo y en el cual las binaras más abiertas sean también más confiables, dada la aparente sensibilidad a éstas. Para 9 de las binarias más abiertas del catálogo encontramos que las velocidades radiales publicadas son concordantes (dentro de las incertidumbres observacionales) para ambas componentes, con lo cual queda establecida su naturaleza física. Estas binarias son muy frágiles y sensibles a las perturbaciones; por ende, son de especial importancia para los modelos dinámicos.

V.3. Simulaciones Monte Carlo.

Estudiamos las interacciones dinámicas con los perturbadores masivos mediante un modelo tipo Monte Carlo, utilizando la aproximación impulsiva y suponiendo un halo galáctico poblado por partículas masivas con una masa dada, de manera análoga al estudio de Yoo et al. (2004) Al igual que estos autores, se desprecian los efectos de la marea galáctica, los encuentros con nubes moleculares la interacción dinámica con el disco galáctico y la posible presencia de binarias recién disueltas en las muestras de binarias observadas.

Provisionalmente, suponemos que la densidad de los perturbadores masivos (MACHOs) es constante, e igual a la densidad local de materia oscura del halo, es decir, $\rho_0 = 0.007\, M_\odot\, pc^{-3}$. Más adelante consideramos el efecto de la dependencia radial de la densidad del halo. El siguiente paso fue calcular el efecto de los 100 encuentros más cercanos en el régimen de marea, y los efectos cumulativos de los encuentros débiles en el régimen de Coulomb. Cada simulación se inicia extrayendo los semiejes de manera uniforme de una distribución que sigue una ley de potencias, con un exponente arbitrario, y con semiejes entre 10 AU y 300,000 AU. Suponemos que la masa de cada

componente de las binarias virtuales es de 0.5 $M_\odot$, y que la distribución de velocidades de los perturbadores es isotrópica, con una dispersión de 200 km s^{-1} en cada componente, lo cual es apropiado para objetos del halo. En cada simulación, hacemos evolucionar a 100,000 binarias durante 10 Giga-años.

Para cada modelo (caracterizado por una masa fija para los MACHOS y una densidad del halo fija) se construye una "matriz de esparcimiento" que nos permite investigar una gran variedad de exponentes para la distribución inicial de semiejes y de valores para la masa de los perturbadores. La matriz de esparcimiento nos da la probabilidad de que una binaria con semieje inicial a_i tenga un semieje final a_f después de 10 Giga-años de evolución. Fijamos la normalización de manera que el número de binarias con semiejes entre a_{min} y a_{max} sea igual al número observado entre esos límites. Este número será distinto para cada submuestra estudiada.

Para obtener los valores del exponente y la masa máxima de MACHOS compatibles con las observaciones, se comienza suponiendo igual a cero la masa de los perturbadores, y se multiplica la matriz de esparcimiento por una ley de potencias, variando el exponente entre -1 y -2 en incrementos de 0.01. Así se encuentra el exponente que da el mejor ajuste a la distribución de semiejes de la muestra estudiada, el cual ajuste estará caracterizado por una dispersión que llamaremos $\sigma = \sigma_0$. A continuación, se repite el procedimiento, ahora variando la masa de los MACHOS en incrementos de 1 $M_\odot$, hasta lograr un ajuste con una $\sigma = 2\sigma_0$ que se considera aún aceptable. De esta manera se obtiene la masa máxima de los MACHOS y la estimación para el exponente de la distribución inicial de semiejes que, después de haber evolucionado durante 10 giga-años, mejor ajusta la distribución observada.

V.4. Resultados.

Con objeto de validar el modelo dinámico, lo aplicamos a la muestra de binarias estudiada por Yoo et al. (2004), y pudimos reproducir sus resultados . También probamos el modelo utilizando la muestra que estudiaron Quinn et al. (2009), es decir, la muestra de Yoo et al. (2004), pero eliminando la falsa binaria. En este caso también pudimos reproducir los resultados publicados (véase la Figura 1 del artículo).

A continuación, aplicamos los modelos a diversas muestras de binarias de nuestro catálogo. Es

necesario recalcar que, a diferencia de otros autores, la comparación se hace directamente sobre los semiejes mayores, estimados en nuestro catálogo a partir de las separaciones angulares observadas, las distancias, y la fórmula teórica de Couteau (1960), que pusimos en a ecuación 2 de este trabajo. Pero también estudiamos el efecto de utilizar la fórmula empírica derivada por Bartkevičius (2008)

$$\langle a \rangle (UA) = \frac{1.3}{\pi} \cdot s'' \qquad (3)$$

basada en datos del "Catalog of Orbits of Visual Binaries" (Hartkopf & Mason 2007) asi como del "Washington Double Star Catalog" (Mason & Hartkopf 2007, Mason et al. 2001, Mason, Wycoff & Hartkopf 2007). Y finalmente reportamos los errores con las cotas obtenidas variando el coeficiente de proporcionalidad en un 20% alrededor del estimado por Couteau (1960). Después de estimar los semiejes esperados de las binarias de la muestra real, los resultados del modelo dinámico se comparan con la distribución de semiejes de distintos grupos de binarias procedentes de nuestro catálogo. Los grupos para la comparación se establecen tomando en cuenta la fracción de su vida que cada sistema pasa en el disco galáctico. Los resultados indican que la distribución inicial que da el límite más conservador para la masa de los MACHOS es la de Oepik para todos los grupos estudiados.

Con objeto de cuantificar los efectos de la densidad no-uniforme del halo galáctico, calculamos valores promediados en el tiempo para la densidad del halo a lo largo de la trayectoria galáctica de cada binaria. Después, calculamos valores promedio sobre todas las binarias del grupo estudiado.

Los resultados que obtuvimos para la masa máxima de los MACHOS calculados aplicando el modelo dinámico a distintas sub-muestras de binarias son los siguientes:

Para la lista depurada de 211 candidatos a estrellas del halo: 112 $M_\odot$.
Para las 150 binarias con órbitas galácticas calculadas: 85 $M_\odot$.
Para las 100 binarias que pasan menos tiempo en el disco (en promedio el 59% de sus vidas): 68 $M_\odot$.
Para las mismas 100 binarias, pero tomando en cuenta la densidad no uniforme del halo: 78 $M_\odot$.
Para las 25 binarias que pasan menos tiempo en el disco (en promedio, el 8% de sus vidas): 11-12 $M_\odot$.

Tomando en cuenta que los experimentos de microlentes establecen que los perturbadores en el halo tienen necesariamente masas menores que 30 $M_\odot$, nuestros resultados prácticamente excluyen la existencia de los MACHOs en el halo galáctico, y hacen necesarias otras explicaciones para, por ejemplo, la curva de rotación plana de la Vía Láctea a grandes distancias galactocéntricas.

VI. Contribuciones específicas del autor al artículo:

"The end of the MACHO era revisited: new limits on MACHO masses from halo wide binaries"

Por Christine Allen & Miguel A. Monroy-Rodríguez

Enviado para su publicación a The Astrophysical Journal. Actualmente en revisión

-Programar y someter a pruebas el modelo para la evolución dinámica de las binarias

-Construir la matriz de esparcimiento y aplicarla a las muestras de Yoo et al. y Quinn et al., con objeto de validar el modelo dinámico.

-Aplicar la matriz de esparcimiento a diversos grupos de binarias

-Comparar los resultados con la distribución observada de semiejes de diversas muestras de binarias del nuevo catálogo

-Obtener los valores para las masas máximas de los MACHOs compatibles con la distribución de semiejes observada para diversos grupos de binarias

-Elaborar todas las gráficas

-Recopilar la bibliografía

The end of the MACHO era- revisited: new limits on MACHO masses from halo wide binaries

Christine Allen[1] & Miguel A. Monroy-Rodríguez[1]

Instituto de Astronomía, Universidad Nacional Autónoma de México, Apdo. Postal 70-264, México, D.F. 04510, México; chris@astro.unam.mx

ABSTRACT

In order to determine an upper bound for the mass of the massive compact halo objets (MACHO's) we use the halo binaries contained in a recent catalog (Allen & Monroy-Rodríguez 2013). To dynamically model their interactions with massive perturbers a Monte Carlo simulation is conducted, using an impulsive approximation method and assuming a galactic halo constituted by massive particles of a characteristic mass. The results of such simulations are compared with several subsamples of our improved catalog of candidate halo wide binaries, which allow us to determine an upper limit of $10 - 12\ M_{\odot}$ for the mass of the MACHOs, based on a 2-sigma estimate of the best fit, corresponding to a 96% confidence level. In accordance with Quinn et al. (2009) we also find our results to be very sensitive to the widest binaries. However, our larger sample, together with the fact that we can obtain galactic orbits for 150 of our systems, allows a more reliable estimate of the maximum MACHO mass than that obtained previously. If we employ the entire sample of 211 candidate halo stars we obtain an upper limit of 112 solar masses. However, using the 150 binaries in our catalog with computed galactic orbits we are able to refine our fitting criteria. Thus, for the 100 most halo-like binaries we obtain a maximum MACHO mass of 68 Mo. Furthermore, we can estimate the dynamical effects of the galactic disk using binary samples that spend progressively shorter times within the disk. By extrapolating the limits obtained for our most reliable -albeit smallest- sample we find that as the time spent within the disk tends to zero the upper bound of the MACHO mass tends to about $12\ M_{\odot}$. The non-uniform density of the halo has also been taken into account, but the limit obtained, $11\ M_{\odot}$, does not differ much from the previous one. Together with studies that provide lower limits on the MACHO mass, our results essentially exclude the existence of such objects in the galactic halo.

Subject headings: binaries: general – dark matter – Galaxy: halo stars: kinematics – stars: statistics

1. Introduction

Disk and halo binaries are relevant to the understanding of processes of star formation and early dynamical evolution. In particular, the orbital properties of the wide binaries remain unchanged after their formation, except for the effects of their interaction with perturbing masses encountered during their lifetimes, as they travel in the galactic environment. The widest binaries are quite fragile and easily disrupted by encounters with various perturbers, be they stars, molecular clouds, spiral arms or MACHOs (massive compact halo objects). For this reason, they can be used as probes to establish the properties of such perturbers. The use of wide binaries as sensors of the dynamical effects of perturbers in the galactic halo has been the subject of several studies (Yoo et al. 1004, Quinn et al 2009). An interesting application of halo wide binaries was proposed by Yoo et al. (2004) who used the catalog of Chanamé & Gould (2004) containing 116 halo binaries to try to detect the signature of disruptive effects of MACHOs in their widest binaries. They were able to constrain the masses of such perturbers to $M < 43\ M_{\odot}$, practically excluding MACHOs from the galactic halo, since a lower limit of about 30 $M_{\odot}$ is found by other studies (Tisserand et al. 2007, Wyrzykowski et al. 2008). However, as was shown a few years later by Quinn et al. (2009) this result depends critically on the widest binaries of their sample, as well as on the observed distribution of the angular separations which, according to Chanamé & Gould, shows no discernible cutoff between 3.5″ and 900″. Quinn et al. (2009) obtained radial velocities for both components of four of the widest binaries in the Chanamé & Gould catalog and found concordant values for three of them, thus establishing their physical nature. The fourth binary turned out to be optical, resulting from the random association of two unrelated stars. Quinn et al. excluded this spurious pair from their study. They assumed a power law distribution for the initial binary projected separation and varied the exponent over a wide range. They evolved the distributions and compared their results with the distribution of the observed projected separations, attempting a best fit of the models to the observed distribution. Quinn et al. found a limit for the masses of the MACHOs of $M < 500\ M_{\odot}$, much less stringent than that previously obtained. They concluded rather pessimistically that the currently available wide binary sample is too small to place meaningful constraints on the MACHO masses. They also pointed out that the density of dark matter encountered by the binaries along their galactic orbits is variable, and that this variation should be taken into account when calculating constraints on MACHO masses.

Motivated by these concerns, we have constructed a catalog of 211 candidate halo wide binaries (Monroy-Rodríguez & Allen 2013), and computed galactic orbits for 150 such binaries. The orbits allowed us to establish the fraction of their lifetime each binary spends within the galactic disk and thus to estimate the dynamical effects of the passage of the binary through the disk. The orbits also allow us to estimate the effects of the variable halo density encountered by the binaries along their galactic trajectories. We stress that for a total of 9 of the widest binaries concordant

radial velocities for both components were found in the literature, thus confirming their physical association. The radial velocities of both components of these pairs were found to be equal within the published observational uncertainties. A more sophisticated analysis was not attempted because the random association of two unrelated stars will most probably result in grossly discrepant radial velocities. Inspection of Table 1 in Quinn et al. (2009) shows that, indeed, the radial velocities of their three physical pairs are equal within the stated uncertainties, whereas the components of the non-physical pair have radial velocities differing by almost 80 km/s.

2. The dynamical model

To model the dynamical evolution of our sample of halo wide binaries we follow closely the procedure of Yoo et al. (2004). In this approach, the impulse approximation is used, and effects of large-scale galactic tides, molecular clouds and dissolved binaries are neglected. We temporarily assume a constant halo density, and attribute to the MACHOs the total local density, taken as $\rho = 0.007\ M_{\odot}/\mathrm{pc}^3$. We then evaluate the effects of the 100 closest encounters in the tidal regime, and compute the cumulative effects of weak encounters in the Coulomb regime. We start the Monte Carlo simulations by drawing initial semiaxes uniformly from a power law distribution with an arbitrary exponent, and with separations between 10 AU and 300 000 AU The mass of each binary component is taken as 0.5 $M_{\odot}$, and the velocity distribution of the perturbers is assumed to be isotropic with a dispersion of 200 km/s in each component, appropriate for halo objects. In each simulation we let 100 000 binary systems evolve for 10 Gy. For each model (with a fixed MACHO mass M and a fixed local halo density), we construct a scattering matrix to simultaneously investigate large sets of initial power law distributions. This scattering matrix gives the probability that a binary with initial semiaxis a will have a semiaxis a' after 10 Gyr of evolution. For each model we fix the normalization so that the number of binaries with major semiaxes between a_{min} and a_{max} is equal to the observed number of binaries within these limits. These limits will be different for the different subsamples used to estimate the maximum MACHO mass. Then, the binary population resulting from the evolved model is compared with the observed sample of binaries.

The goodness of fit is evaluated computing the dispersion, σ. We should stress that the simulated and the observed binary samples are compared directly, but compare the evolved distribution of stars in each bin of the observed major semiaxis distribution, attempting a best fit to this distribution. Previous work (Yoo & Chaname, Quinn et al. 2009) fitted the observed projected separations. Also, since distances are available for all our binaries, we prefer to compare directly the resulting model distribution of major semiaxes with the observed one, calculated from the angular separations and the individual distances. Projection effects are taken into account by means of the widely

used statistical formula (Couteau 1960):

$$\langle a'' \rangle = 1.40 s''.$$

This formula was derived theoretically, and includes the eccentricity distribution of the binaries, as well as projection effects. Here, $\langle a \rangle$ represents the expected value of the major semiaxis a and $\langle s \rangle$ or that of the angular separation s. A recent empirical study (Bartkevicius 2008) compares the angular separations with the major semiaxes for systems from the Catalog of Orbits of Visual Binaries (Hartkopf & Mason 2007). The results obtained vary somewhat according to the data used for the separations s from "first" or "last" observations in the WDS (Mason et al. 2001) , or from the orbit catalog ephemerides, the latter deemed to provide the most reliable value, namely:

$$\log\langle a \rangle - \log s = 0.112.$$

In spite of the rather large uncertainties of the latter values, we shall use both estimates to compute the maximum MACHO masses.

To obtain the values of the exponent and the maximum MACHO mass compatible with the observations we proceed as follows. We start by assuming the mass of the perturbers to be zero, and multiply the scattering matrix by power laws, letting the exponent vary between -1 and -2 (in increments of 0.01), until the best fit to the observed distribution is found.. This fit is characterized by a $\sigma = \sigma_0$. Then we repeat the procedure, increasing the perturber mass in increments of 1 $M_\odot$, until a fit is obtained with a $\sigma = 2\sigma_0$, which we take as still acceptable. This yields the maximum MACHO mass still compatible (within $2\sigma_0$) with the obsevations.

As an illustration, Figure 1 shows our results for the group of 100 most halo-like binaries, compared to the obseved sample. The frequency distribution of expected semiaxes is plotted in the vertical axis. The large squares indicate the observed distribution. The horizontal dotted line corresponds to an unevolved binary population with a power law exponent of -1. The dashed line shows the optimum fit to the obseved distribution and yields a MACHO mass of 37 $M_\odot$. Let the dispersion of this fit be σ_0. To obtain a maximum MACHO mass, we fit the model again, but allowing a dispersion of twice the value for the optimum fit, that is, $2\sigma_0$. The overall fit thus obtained is still reasonable, but the maximum MACHO mass increases to 68 $M_\odot$. The figure also shows that the horizontal line (exponent -1) represents the initial -unevolved- distribution which has to evolve farthest in order to fit the observed distribution, that is, that which needs the largest mass of perturbers to conform with observations. In this sense, taking an initial distribution with a -1 exponent yields the most conservative estimate for the perturber mass, i.e. the largest MACHO mass. Furthermore, as pointed out by also by Quinn et al., there are both theoretical and observa-

tonal reasons to justify the assumption of an exponent −1 for the unevolved distribution. Indeed, Valtonen (1997) showed Oepik's distribution to correspond to dynamical equilibrium, and it has been found to hold for many different samples of wide binaries of different ages and provenances (Poveda et al. 2006, Sesar et al. 2008, Lepine & Bongiorno 2007, Allen et al. 2000). In the accompanying paper (Monroy-Rodríguez & Allen 2013) we show that it holds for halo binaries up to different limiting semiaxes, according to the time the binaries spend within the galactic disk. For the most halo-like binaries, it holds up to expected semiaxes of 63,000 AU.

The range of exponents considered for the power law distribution amply covers the observationally found ones. So, for example, Chanamé & Gould (2004) find −1.67 and −1.55 for their disk and halo binaries, repectively. Sesar et al. (2008) find −1; Lepine & Bongiorno (2007) obtain −1; Poveda et al. (1994, 1997, 2003, 2004) find -1 but up to different limiting semiaxes according to the age of the binaries; finally, Allen et al. (2000) find −1 for their high-velocity metal-poor binaries, but also only up to different limiting semiaxes, according to the time spent by the binaries within the galactic disk.

The results are dependent on the definition of σ, we have preferred to generate a virtual binary sample with the same number of binaries as that of the observed sample and then to calculate the σ as the ordinary standard deviation of the semimayor axes using the linear scale of separations, instead of calculating an error using the logarithmic scale of fitted separations, as was done by Yoo et al. and Quinn et al. The 2σ fits correspond to a confidence level of 95.4%.

The best fit between the model distribution and the observed one fixes the value of M, the mass of the perturbers. As explained above, the most conservative estimate (largest MACHO mass) is obtained for an exponent of −1, which corresponds to the Oepik distribution.

Our implementation of the dynamical model was tested by applying it to the binary samples studied by Yoo et al. (2004) and Quinn et al. (2009). As shown in Figure 2, we were able to closely reproduce their results, and thus consider our model as validated.

3. Application to the improved catalog of candidate halo binaries

We are now ready to apply our dynamical model to different subsets of binaries extracted from our catalog (Monroy-Rodríguez & Allen 2013). For this study we consider mainly the 150 binaries with computed galactic orbits. The galactocentric orbits were integrated using the standard 1991 Allen & Santillan (axysimmetric) galactic potential. Since very few orbits approach the zone of influence of the bar, an axisymmetric potential was found to be adequate. The orbits were integrated backwards in time for 10 Gyr. The relative energy error amounted to less than 10^{-7} at the end of the integration. To establish membership to the halo we calculate the time the binary

spends within the galactic disk (±500 pc). In Table 1 we display our main results. The different samples of binaries listed in Column 1 are ordered by the time they spend in the disk. Thus, the first entry corresponds to the 25 most halo-like binaries, which spend an average of only 0.08 of their lifetimes in the disk. The second column lists the fraction of their lifetimes the binaries spend in the disk. Column 3 displays the upper limits obtained for each group of binaries, with the fits performed to 2σ, so as to be able to compare these results with the ones obtained by Quinn et al. Column 4 shows the limits obtained taking into account, on average, the variable halo density encountered by the binaries along their galactic trajectories. We shall further discuss these entries in the next sections.

4. Estimate of the dynamical effect of the disk

We still have to take into account the dynamical interactions that the binaries experience during their passage through the galactic disk. These effects have not been considered in previous studies (Yoo et al. 2004; Quinn et al. 2009). At this stage, we shall not attempt a full dynamical modeling, but instead roughly estimate the effects of the disk passages by studying groups of binaries that spend progressively smaller fractions of their lifetimes within the disk. The result of this estimate is shown in Figures 3 and 4 where we display the MACHO masses obtained by applying the dynamical model to the groups of binaries displayed in Table 1. Taking the last point in the graph, we find a maximum MACHO mass of about 12 $M_{\odot}$. We remark that the smallest group, the 25 most halo-like binaries includes 6 very wide systems with concordant radial velocities, as reported in the literature. Therefore, their physical association can be considered as established. Five of these binaries are among the widest known, and thus particularly suitable for determining upper limits to the masses of the perturbers. Since the 25 most halo-like binaries form a very interesting group for further studies (especially, for determining the radial velocities of both components, and thus confirming -or not- their physical nature), we list them in Table 2, along with their main characteristics.

Columns 1 and 2 contain the designation of the primery and secondary components, respectively, Column 3 lists our adopted distance. Columns 4 and 5 display the absolute visual magnitudes of the primary and secondary, respectively. Column 6 lists the projected separation in arcsec, Column 7 the expected value of the major semiaxis in AU. Column 8 displays the peculliar velocity of the binary, and Columns 9, 10 and 11 the main characteristics of its galactocentric orbit, namely, the maximum distance from the galaxtic center, the maximum distance from the galactic plane, and the eccentricity, respectively. In the last column we list the fraction of its lifetime spent by the binary in the galactic disk, that is, within $z = \pm 500$ pc.

5. Estimate of the effect of considering a non-uniform halo density

As was already pointed out by Quinn et al. the density of the halo cannot be assumed to be uniform. This is particularly relevant for galactic orbits that reach large apogalactic distances or large distances from the plane. To obtain a rough estimate of the effect of this non-uniform density on the computed mass limits, we calculated for each binary a time-averaged halo density over its galactic orbit. Then, we averaged over the binaries in each studied group. The average densities turned out not to be very different from the density at the solar distance. This is due to the fact that, since the sample of binaries is restricted to nearby stars, orbits that reach large apogalactic distances also penetrate close to the galactic center, where they encounter large densities. Only a few binaries reaching large $z-$distances encounter considerably smaller average halo densities. As an aside, we point out that our orbit for NLTT 10536/10548 differs significantly from that plotted by Quinn et al. Our orbit reaches a $z_{\max}$ of only 5.2 kpc, instead of the almost 40 kpc in Quinn et al. This may partially account for the differences in the average halo densities found by us, which are much less significant than those obtained by the former authors. The result of estimating the effects of a variable halo density is shown in Figure 5, for the groups of binaries of Table 1. The Figure 6 shows the mass limits obtained as a function of the fraction of time spent in the disk for each group, for the averaged densities as described above and can be compared with Figure 4. The fits to obtain the limiting masses were performed to 2σ (which corresponds to a confidence level of 96%) . From the last point in the graphs it is seen that the limiting masses obtained are about 10 to 12 $M_{\odot}$. If we extrapolate to zero time spent in the disk we see that the maximum MACHO decreases to less than 10 $M_{\odot}$.

If instead of using the Couteau (1960) formula for transforming observed separations into expected major semiaxes we use the expression derived by Bartkevicius (2008) we obtain the results shown in Table 3. The table shows that the derived limits increase somewhat, but this increase (on average about 5%) does not significantly alter the main conclusions of this study.

The individual distances to the binaries used to convert separations in arcsec into separations in AU and then into expected major semiaxes have, of course observational uncertainties. Since the groups of binaries we use to determine maximum MACHO masses contain binaries from different sources, we can only provida an estimated average uncertainty for the distances, trying to err on the conservative side. In our catalog, we adopted the distances given in the Hipparcos catalog when their parallax errors were less than 15%, Otherwise we adopted, in order of preference, the Strömgren photometric distances given in the lists of Nissen & Schuster (1991) , those obtained with the polynomial of Chaname & Gould, using their photometry, or the spectroscopically derived distances of Ryan (1992) and Zapatero-Osorio & Martin (2004). Most of our binaries should have distance errors of about 15%. Since we order our binaries by the time they spend within the disk, only average values of the distance uncertainties can be given for each group. These averages

translate into average uncertainties in the expected major semiaxes. We re-computed the dynamical models to obtain a best fit to the distances with probable errors of 20% added and subtracted to the expected semiaxes. We used these results to determine the error bars now shown in the figure 7. On average the maximum MACHO masses vary by about 20% , somewhat more than they do by adopting two alternative formulae for transforming the observed linear separations into expected major semiaxes.

6. Summary and conclusions

From a catalog of 251 candidate halo wide binaries we have extracted different subgroups in order to determine upper bounds to the MACHO masses. For a group of 150 binaries it was possible to compute galactic orbits and thus to evaluate the time they spend within the galactic disk. We developed and validated a dynamical model for the evolution of wide halo binaries subject to perturbations by MACHOs. This model was applied to different subsamples from the catalog , thus allowing us to obtain as upper limits for the masses of MACHOs the following values:

From 211 systems most likely to be halo binaries: 112 $M_{\odot}$.

From 150 halo binaries with computed galactic orbits: 85 $M_{\odot}$.

From 100 binaries that spend the smallest times within the disk (on average, half their lifetimes): 68 $M_{\odot}$.

From the same 100 binaries, but taking into account the non-uniform halo density: 78 $M_{\odot}$.

From the 25 most halo like binaries (those that spend on average 0.08 of their lifetimes within the disk): $11 - 12\ M_{\odot}$

MACHOs have been a strong candidate for the dark matter that appears to dominate the mass of galaxies, at least at large radii. Microlensing experiments (Tisserand et al. 2007, Wyrzykowski et al. 2008) exclude baryonic MACHOs with masses in the range 10^{-7} to 30 $M_{\odot}$ as dominant constituents of the dark matter halo. Other studies (Lacey & Ostriker 1985, Rújula et al. 1992) have ruled out MACHO masses larger than about 10^{6} $M_{\odot}$. Wide binaries, as studied by Yoo et al. restricted the range of possible MACHO masses to $30 - 45\ M_{\odot}$, but their results were shown by Quinn to critically depend on one of their widest binaries, which turned out to be spurious. Excluding this binary, Quinn et al. found a less stringent upper limit of about 500 $M_{\odot}$.

In the present study we have used an expanded catalog of candidate halo wide binaries to revise the limits for the MACHO masses. From different subsamples of binaries we obtain maximum MACHO masses ranging from 112 $M_{\odot}$ all the way down to less than 10 $M_{\odot}$, The most

stringent limits are obtained from the most halo-like sample of 25 wide binaries, a sample particularly suited for further studies. These results, once again, all but exclude the existence of MACHOs in the galactic halo.

REFERENCES

Bartkevičius, A. 2008, Baltic Astronomy, 17, 209

Chanamé, J. & Gould, A. 2004, ApJ, 601, 289

Couteau, P. 1960, J. des Observateurs, 43, 41

De Rújula A., Jetzer P., & Massaó E., 1992, A&A, 254, 99

Hartkpof, W. I., & Mason B. D., 2007, Sixth Catalog of Orbits of Visual Binary Stars, WDS06, U.S. Naval Observatory, Washington

Lacey, G. C., & Ostriker, J. P. 1985, ApJ, 299, 633

Mason, B. D., Wycoff, G. L., Hartkopf, W. I., Douglass, G. G., Worley, C. E., 2001, AJ, 122, 3466

Mason, B. D., & Hartkopf, W. I., 2007, IAUS, 240, 575

Monroy-Rodríguez, M.A. & Allen, C. 2013,ApJ, in press

Quinn, D. P., Wilkinson, M. I., Irwin, M. J., Marshall, J., Koch, A. and Belokurov V. 2009, MNRAS, 396, L11

Tisserand, P. et al., 2007, A&A, 469, 387

Wyrzykowski, L. et al., 2009, MNRAS, 397, 1228

Yoo, J., Chanamé, J. & Gould, A. 2004, ApJ, 601, 311

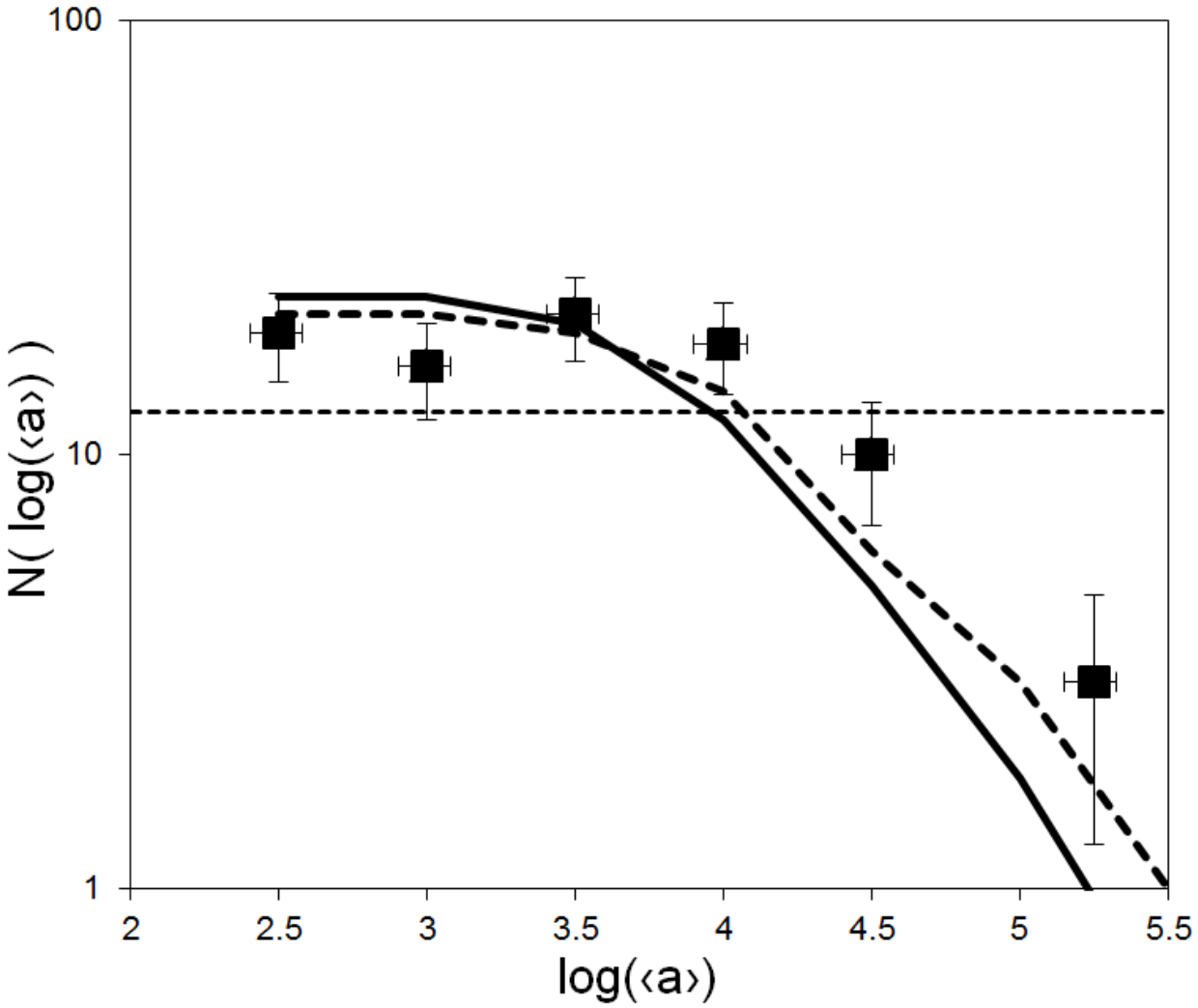

Fig. 1.— Results for the 100 most halo-like binaries, compared to the obseved sample. The large squares indicate the observed distribution. The horizontal dotted line corresponds to an unevolved binary population with a power law exponent of −1. The dashed line shows the evolved population that best fits the observations and corresponds to a MACHO mass of 37 $M_{\odot}$. The solid line shows the evolved population with a maximum MACHO mass of 68 $M_{\odot}$.

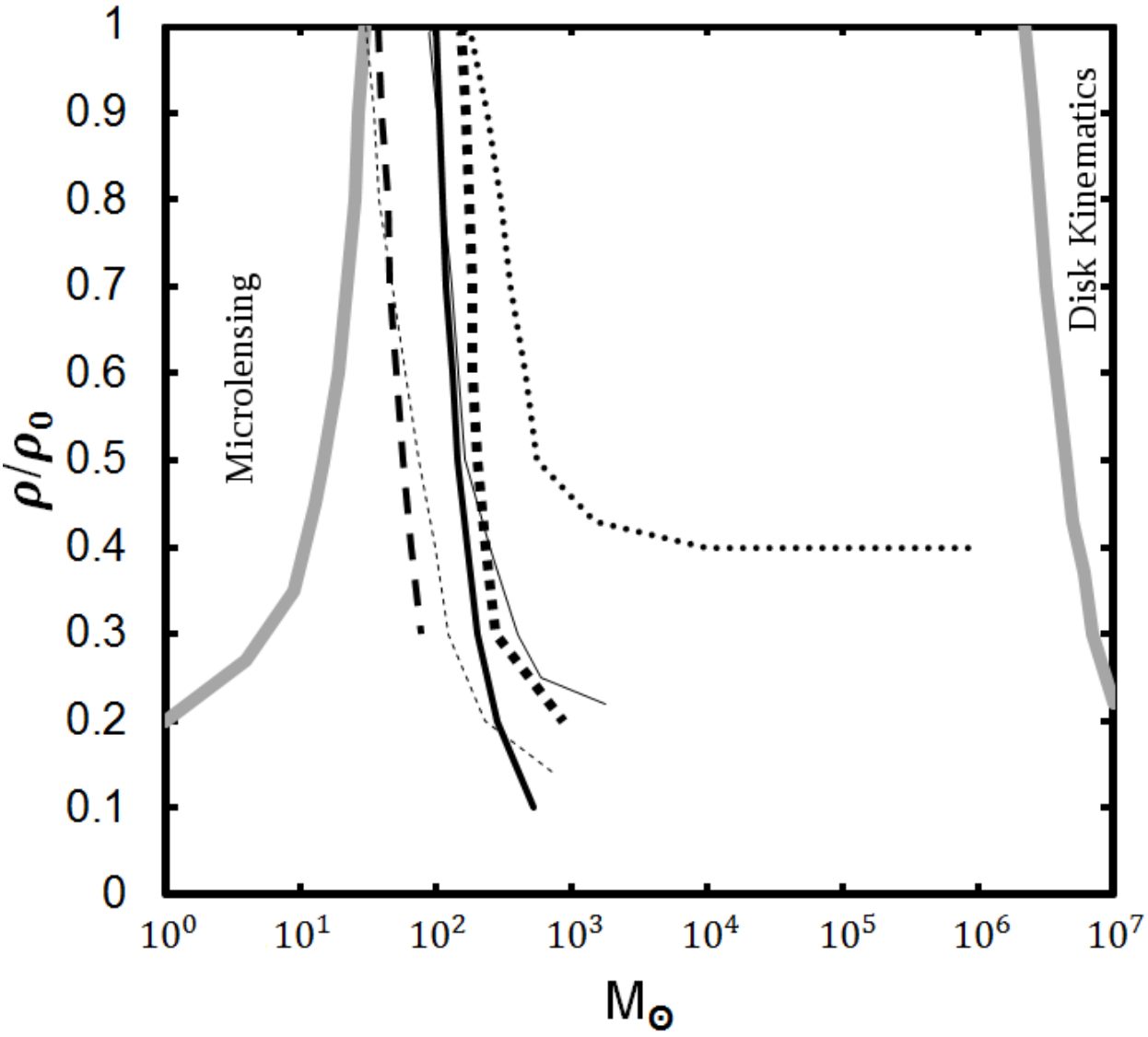

Fig. 2.— Confidence regions for the MACHO mass M_p and the MACHO halo fraction. Our results are overplotted on the graph by Quinn et al. The dashed line result from using the sample of Yoo et al. and ji-square error. They are seen to closely reproduce Yoo et al.'s result for a halo fraction of 1. The straight line display the result we obtain by applying our dynamical model to the sample of Yoo et al,. but using a 2σ fitting criterion. We closely reproduce Quinn et al.'s results. Finally, the square dots represent our results for the same sample, but omitting the spurious pair, Again, we closely reproduce Quinn et al.s results, especially for halo fractions larger than 0.4, which encompass the region of interest.

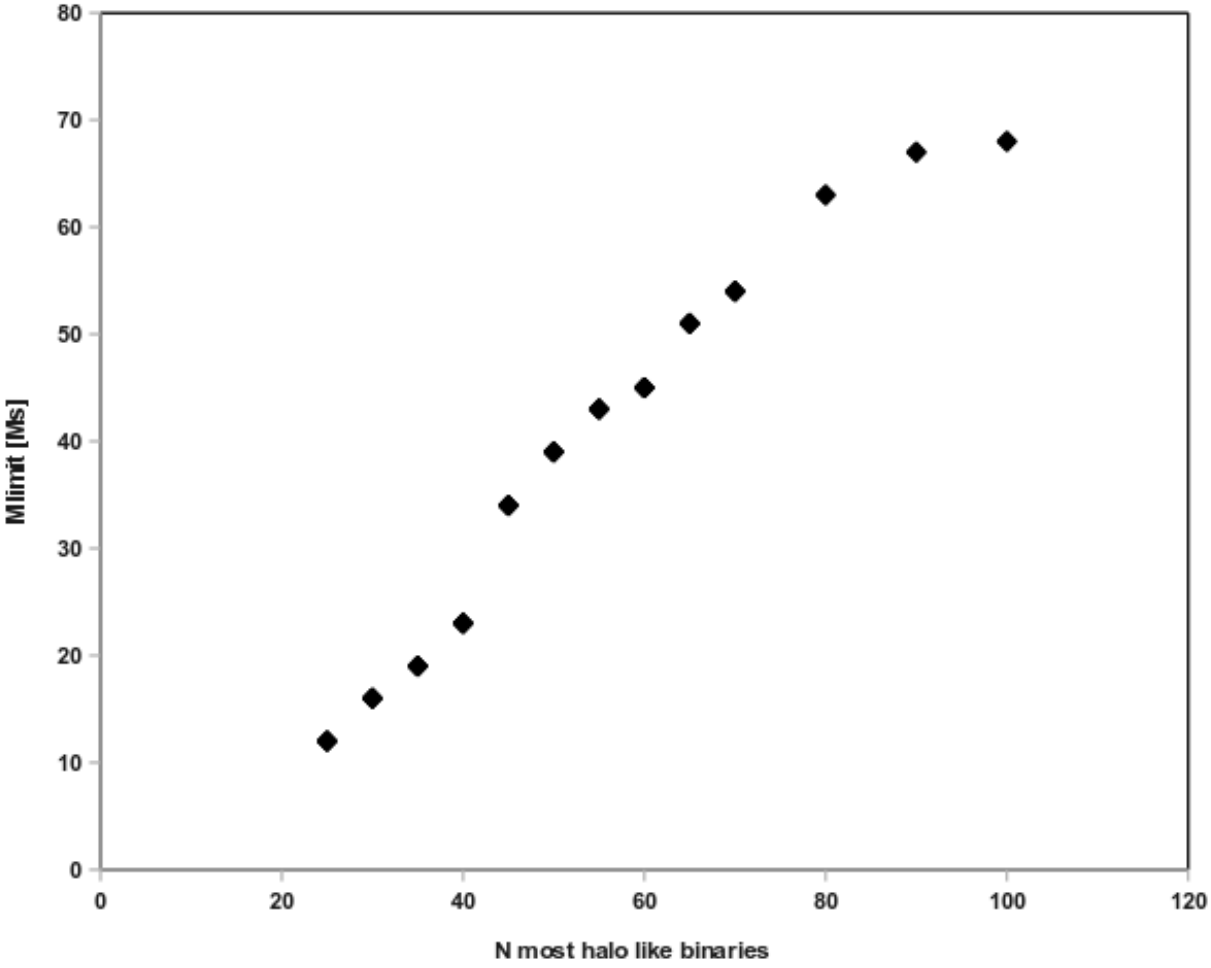

Fig. 3.— Maximum masses for MACHOs obttained by applying our dynamical model to the different groups of binaries listed in Table 1, as a function of the number of most halo-like binaries in the sample. A constant halo density is assumed.

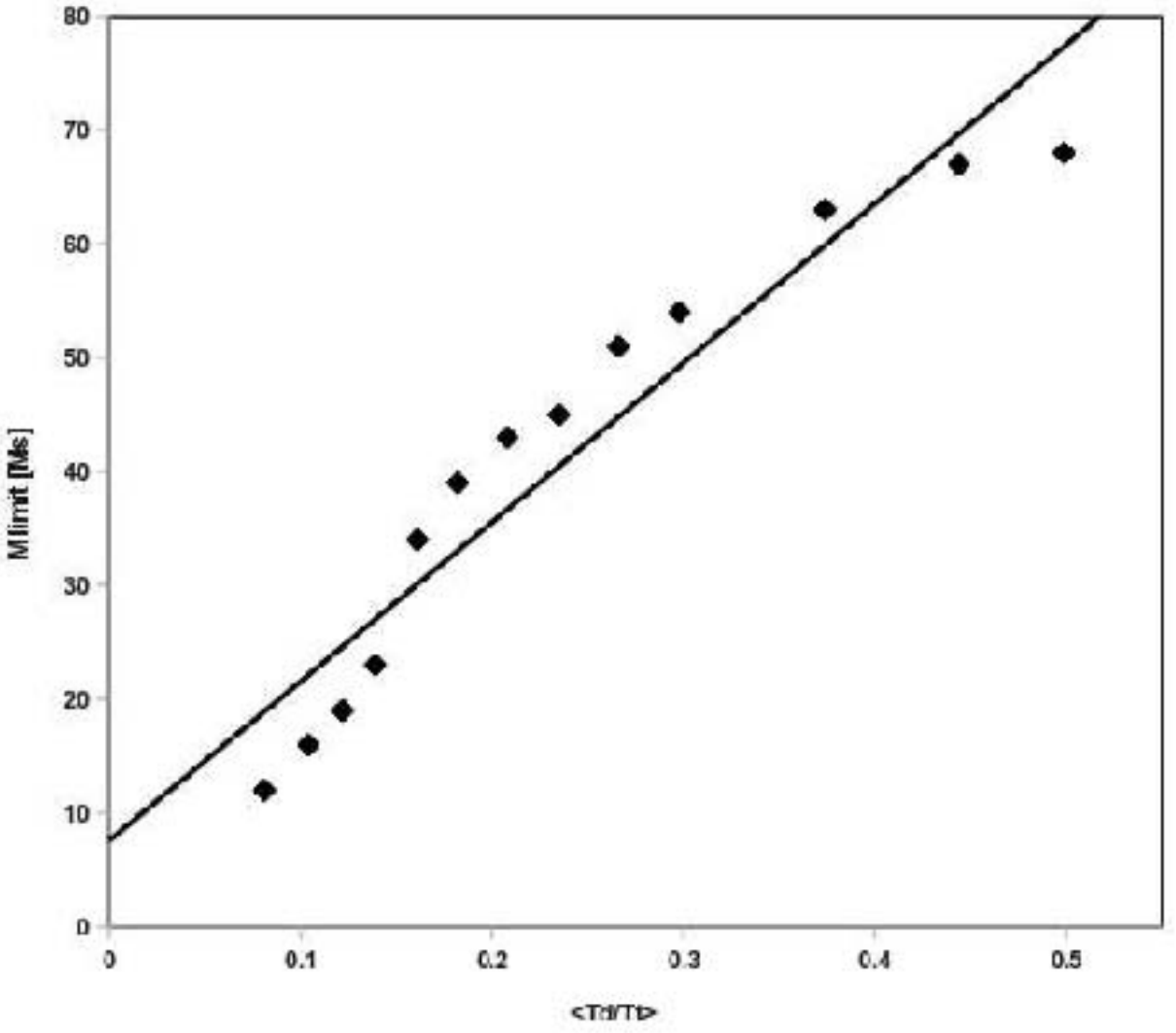

Fig. 4.— Same as Figure 3, but plotted in terms of the time spent by the binaries within the galactic disk. The extrapolation to zero time spent in the disk would imply a maximum MACHO mass below 10 $M_{\odot}$. A constant halo density is assumed.

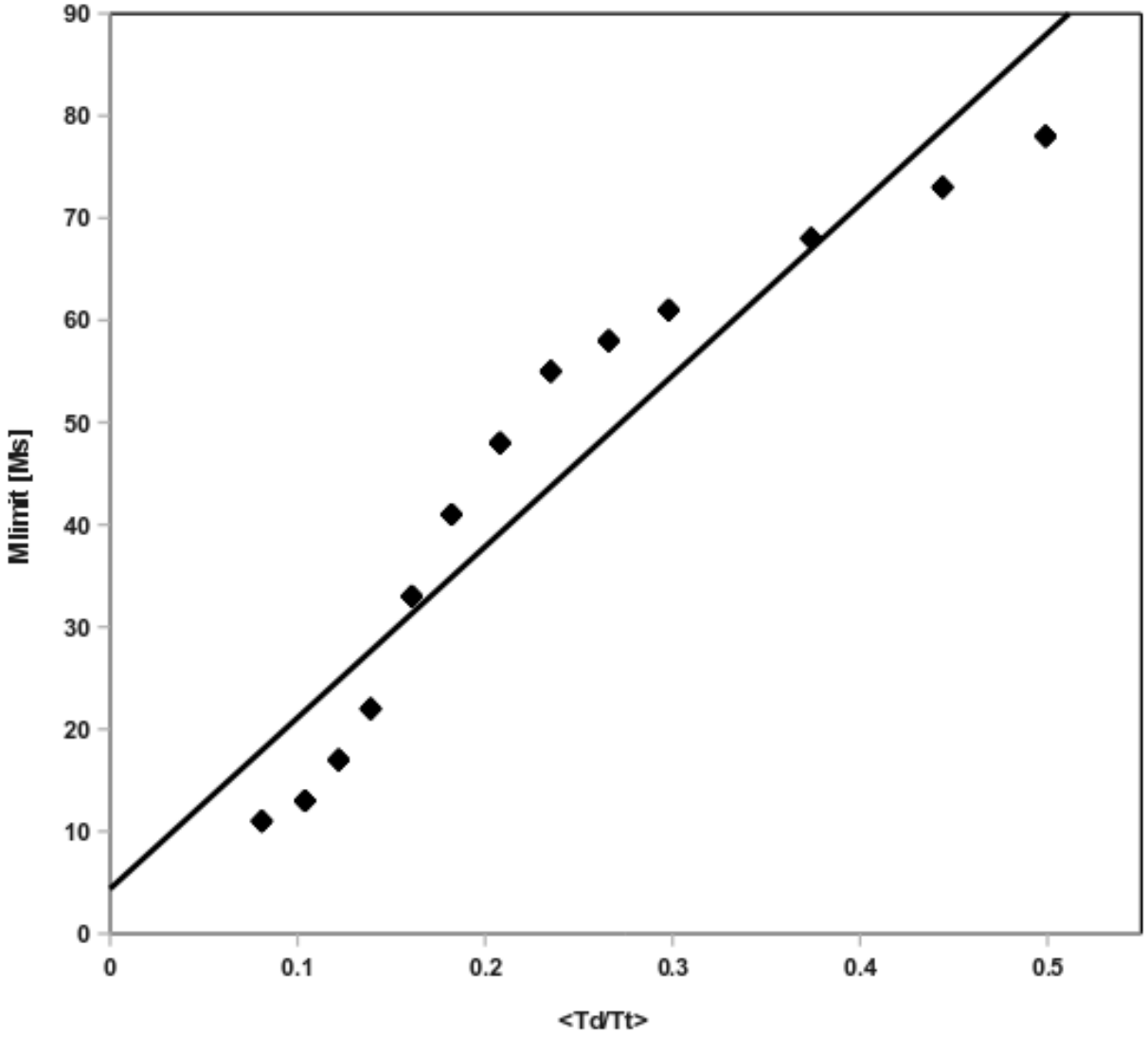

Fig. 5.— Same as Figure 4, but taking into account the non-uniform halo density encountered by the binaries along their galactic trajectories. The extrapolation to zero time spent in the disk would imply a maximum MACHO mass well below 10 $M_{\odot}$.

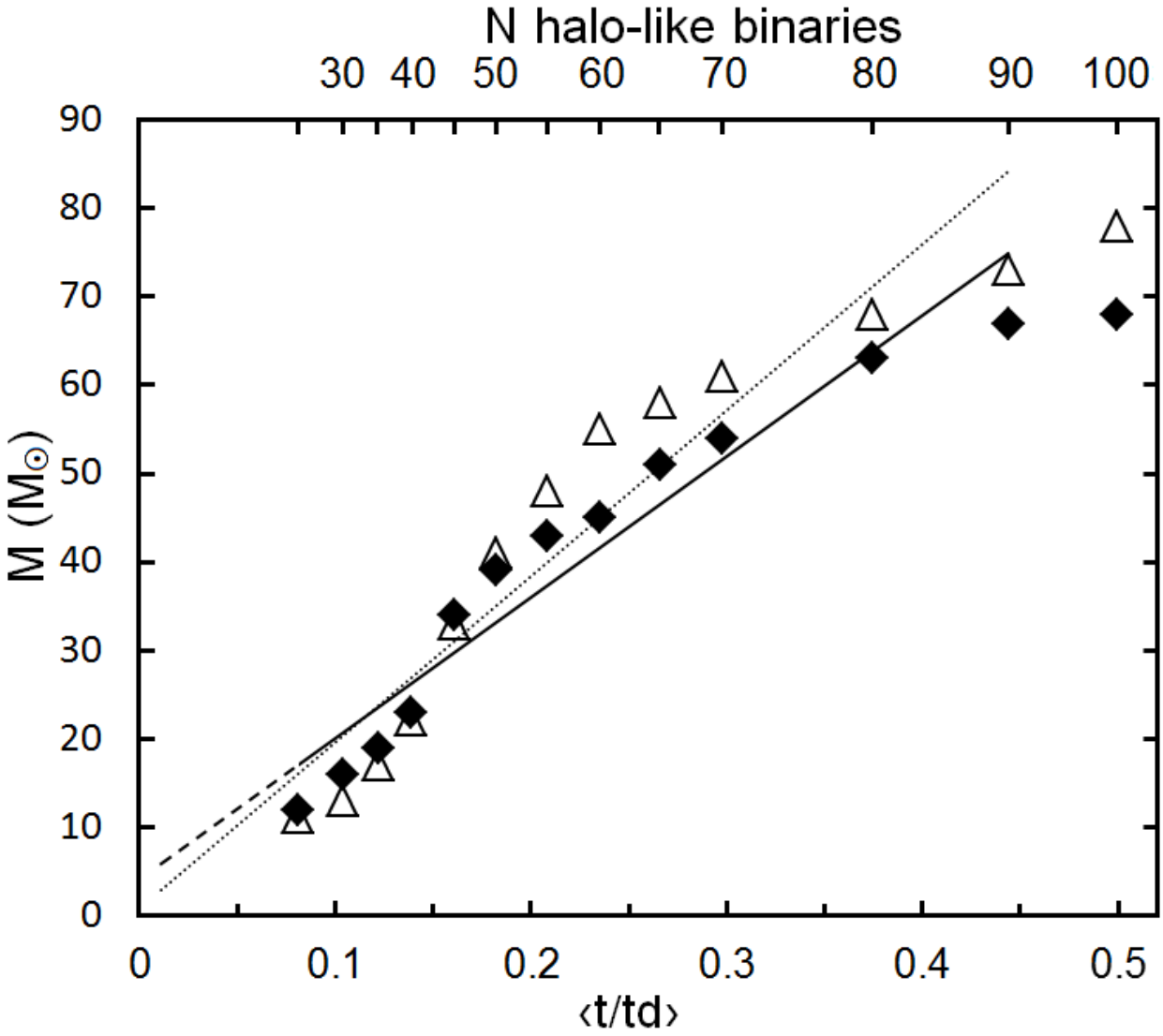

Fig. 6.— Maximum masses for MACHOs obttained by applying our dynamical model to the different groups of binaries listed in Table 1, as a function of the time spent by the binaries within the galactic disk. Comparison of the results obtained using the local density of dark matter (black rhombs), with the results obtained with average densities by sample (white triangles).

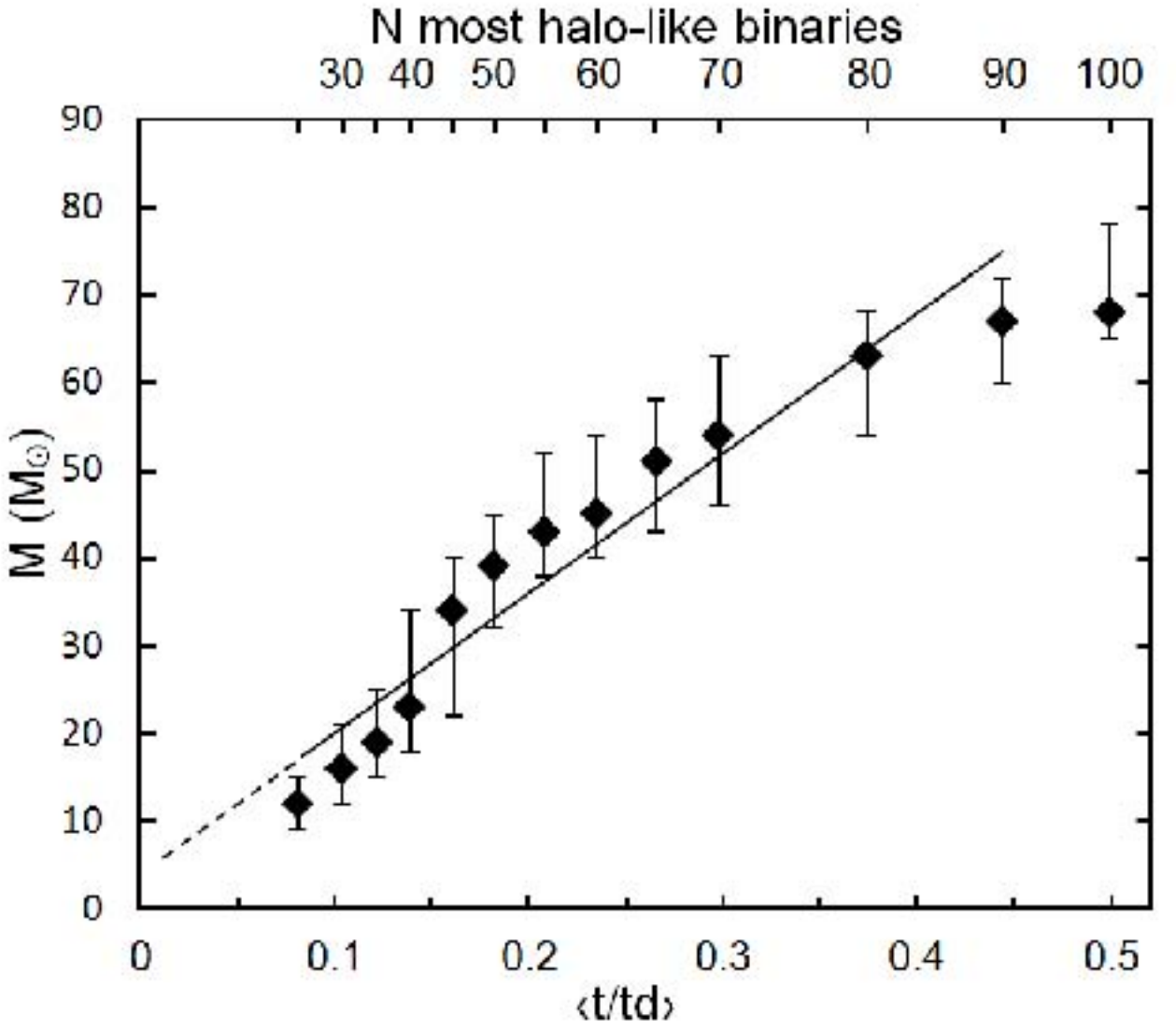

Fig. 7.— Error bars shown the variation of the limit masses of the MACHOs considering a 20% of error in the expected semiaxes calculated with Couteau's formula.

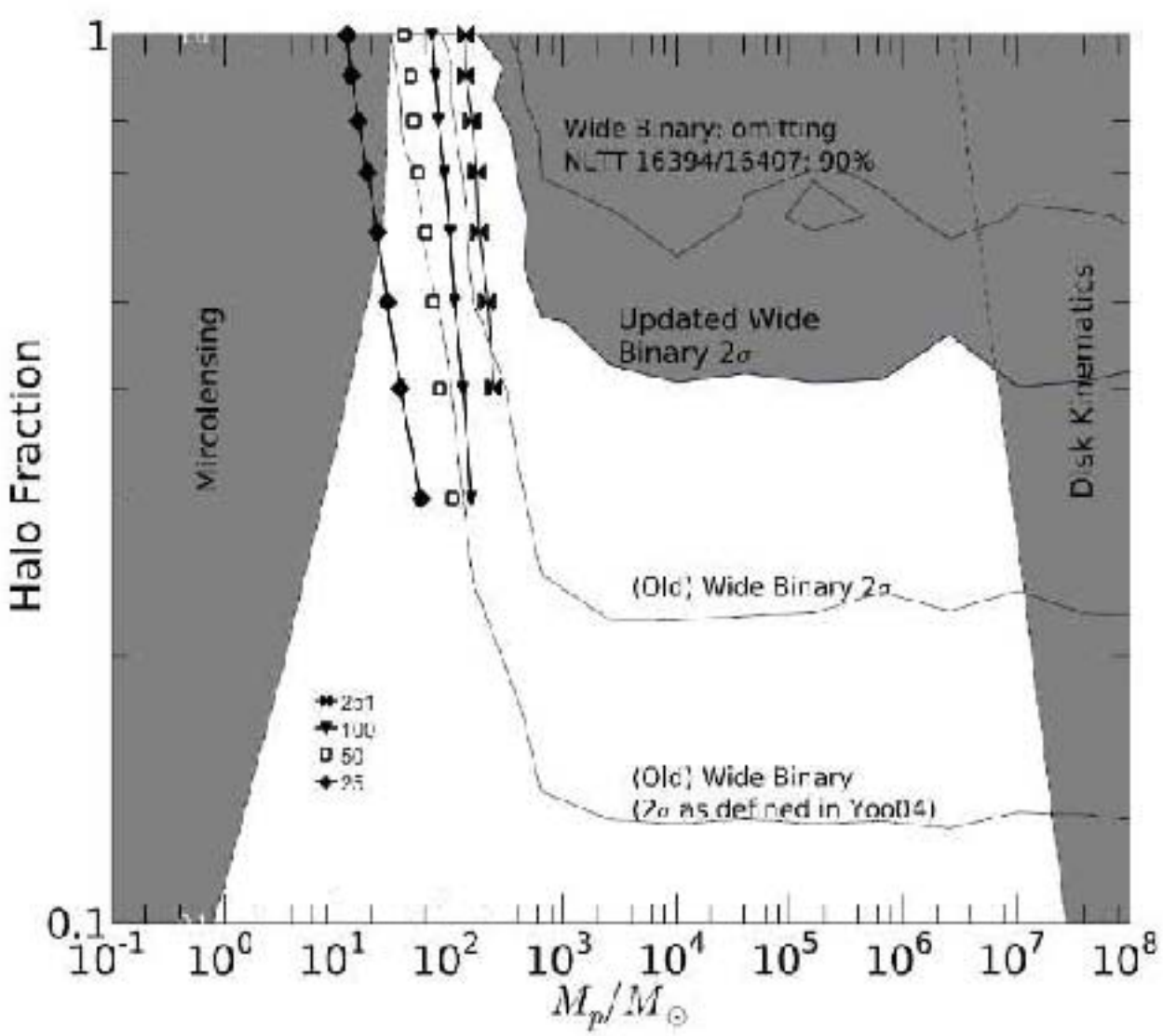

Fig. 8.— Confidence regions for tha MACHO mass M_p and the MACHO halo fraction overplotted on the Quinn et al. graph, for easy comparison. Results for different groups of binaries are shown by different symbols, corresponding respectively to the full sample of 251 candidate halo binaries, to the 100, 50 and 25 most halo like samples, according to successively smaller times spent within the disk galactic.

Table 1: Upper limits for the mass of the Massive Compact Halo Objets (MACHO's).

$Sample$[a]	$\langle T_d/T_t \rangle$	$M(\rho_0)$ $[M_\odot]$	$M(\langle\rho\rangle)$ $[M_\odot]$
25	0.08	12	11
30	0.10	16	13
35	0.12	19	17
40	0.14	23	22
45	0.16	34	33
50	0.18	39	41
55	0.21	43	48
60	0.24	45	55
65	0.27	51	58
70	0.30	54	61
80	0.37	63	68
90	0.44	67	73
100	0.50	68	78
Yoo[b]		80	
Quinn[c]		105	

[a] Number of the most halo like binaries with computed galactic orbits

[b] 90 halo binaries of Chaname and Gould 2004

[c] The sample used by Quinn et al. eliminating one spurious binary

Table 2. The 25 most halo like wide binaries

Primary	Secondary	d (pc)	M_V(p)	M_V(s)	s (")	$\langle a \rangle$ (AU)	v_p (km/s)	$R_{\rm max}$ (kpc)	$\lvert z_{\rm max} \rvert$ (pc)	e	td/t
(1)	(2)	(3)	(4)	(5)	(6)	(7)	(8)	(9)	(10)	(11)	(12)
NLTT 16394*	NLTT 16407*	348	4.5	7.6	698.5	340309	481.5	144.0	88786	0.90	0.003
NLTT 37787	NLTT 37790	193	9.9	6.4	200.9	54283	470	115.2	109015	0.92	0.003
NLTT 4814	NLTT 4817	153	10.7	5.2	24.4	5139	303	12.9	8058	0.98	0.006
NLTT 5781	NLTT 5784	306	11.6	7.1	52.1	22320	380.4	44.2	32637	0.91	0.019
NLTT 18775	G090-036B	293	5.4	8.8	1.67	685	515.8	429.1	53116	0.96	0.020
NLTT 18346*	NLTT 18347*	167	5.1	4.3	11.9	2805	290.3	21.6	17469	0.52	0.028
NLTT 49562*	G 262-022r*	281	6.7	7.2	29.54	12155	370.5	40.0	27828	0.98	0.031
NLTT 1036	NLTT 1038	290	10.8	6.0	22.5	9135	213	9.8	7363	0.29	0.049
NLTT 32187	VBS 2	80	3.8	7.8	1.9	213	356.1	22.0	9995	0.94	0.055
NLTT 41756	VB 6	256	6.3	8.7	1.5	537	515.9	19.9	6958	0.43	0.060
NLTT 10536*	NLTT 10548*	214	4.6	9.1	185.7	55410	417.5	9.6	5202	0.12	0.062
NLTT 43097*	G 017-027j*	48	6.2	10.5	1170.7	79139	162.7	9.4	5692	0.69	0.074
NLTT 39442	LP 424-27	132	6.4	6.6	677	125073	306.7	15.6	7088	0.87	0.075
NLTT 5690	LP 88-69	71	4.1	9.1	22	2198	183.7	8.6	4562	0.51	0.083
NLTT 39456*	NLTT 39457*	29	6.7	7.1	300.7	12380	592.2	67.0	6410	0.86	0.088
NLTT 16062	BD 34 567	70	6.6	10.4	12	1176	265.5	11.8	6401	0.94	0.103
NLTT 9798	LP 470-9	100	3.6	7.6	1	140	104.5	8.7	2366	0.10	0.121
NLTT 52786	NLTT 52787	167	5.8	5.3	2	468	162.4	9.7	3623	0.58	0.123
NLTT 16629	NLTT 16631	55	6.4	10.5	434.1	33416	179.6	8.9	2562	0.29	0.125
NLTT 19979	NLTT 19980	344	7.9	10.2	19.6	9439	228.1	15.0	8120	0.92	0.135
NLTT 38195	BD+06 2932B	73	6.1	9.0	3.6	443	267.6	18.1	10301	0.96	0.137
NLTT 51780	G093-027B	136	6.0	8.7	3.52	672	259.8	14.4	2596	0.45	0.149
NLTT 525	NLTT 526	251	4.8	7.4	8.5	2986	361.3	31.6	3122	0.92	0.157
NLTT 14005	NLTT 13996	103	5.7	12.6	133	19173	101.9	8.7	2000	0.20	0.157
NLTT 17770	LP 359-227	180	4.1	10.4	34	8565	262.7	11.7	8661	0.96	0.158

*wide binaries with concordant radial velocities.

Table 3. Comparison of upper limits to the MACHO masses using two estimates for $\langle a \rangle$, for a constant halo density.

$Sample$[a]	Couteau $M(\rho_0)$	Bartkevicius $M(\rho_0)$
25	12	13
30	16	17
35	19	20
40	23	25
45	34	34
50	39	40
55	43	44
60	45	49
65	51	52
70	54	57

[a]Number of the most halo-like binaries with computed galactic orbits.

VI. Resumen y conclusiones

Hemos elaborado un nuevo catálogo con 251 candidatos a binarias abiertas del halo galáctico, y hemos calculado órbitas galácticas para 150 de ellas. Las órbitas galácticas permiten calcular el tiempo que cada binaria pasa en el disco galáctico, y con ello, pueden ordenarse según la fracción de sus tiempos de vida durante las cuales están sujetas solamente a las perturbaciones del halo. Esta fracción es importante para los modelos dinámicos.

La distribución de los semiejes esperados de las binarias de nuestro catálogo es claramente tipo Oepik, pero hasta semiejes límite que dependen de la fracción de sus vidas que las binarias pasan en el disco. Estos resultados se han obtenido mediante la aplicación de la prueba de Kolmogorov-Smirnov a distintas muestras de binarias del catálogo. Para el grupo de 50 binarias que más tiempo pasa en el disco, la semieje límite es de 15,000 AU, para las 50 que pasan menos tiempo en el disco el semieje límite es de 63 000 AU.

Hemos modelado la evolución dinámica de las binarias abiertas mediante un método Monte Carlo que, aplicado a 100 000 binarias virtuales, nos permitió obtener la "matriz de esparcimiento", la cual nos da la probabilidad de que una binaria con semieje inicial a tenga un semieje a' después de 10 Giga-años de evolución. El modelo calcula los efectos perturbativos de los 100 encuentros más cercanos en el régimen de marea, y evalúa el efecto acumulado de encuentros más lejanos en el régimen de Coulomb. El modelo fue validado aplicándolo a las muestras de binarias estudiadas por Yoo et al. (2004) por Quinn et al. (2009), cuyos resultados pudieron ser reproducidos.

Los límites que obtenemos para las masas máximas de los MACHOs son menores y más confiables que los obtenidos por otros autores. Nuestro resultado para los grupos de binarias que menos tiempo pasan en el disco es de 11-15 $M_{\odot}$. Este resultado prácticamente excluye la existencia de los MACHOs en el halo galáctico

IX. Bibliografía

Afonso, C., Albert, J. N., Andersen, J. et al. 2003, A&A, 400, 951

Alcock, C., Allsman, R. A., Alves, D. R. et al. 2001, ApJ, 550, L169

Alcock, C. Allsman, R.A. Alves,D. et al. 1998, ApJ, 499, L9

Allen, C. & Monroy-Rodríguez, M.A. 2013, ApJ, submitted

Allen, C. & Poveda, A. 2007, in Binary Stars as Critical Tools & Tests in Contemporary Astrophysics, IAU Symposium 240, Eds. W.I. Hartkopf, E.F. Guinan and P. Harmanec. Cambridge: Cambridge University Press, p. 405

Allen, C., Poveda, A. & Herrera, M. A. 1997, in Visual Double Stars : Formation, Dynamics and Evolutionary Tracks. J.A. Docobo, A. Elipe, and H. McAlister. Dordrecht: Kluwer Academic, ASSL. 223, p. 133

Allen, C., Poveda, A. & Herrera, M.A. 2000, A&A, 356, 529

Allen, C. & Santillán, A. 1991, RMxAA 22, 255

Bartkevičius, A. 2008, Baltic Astronomy, 17, 209

Chanamé, J. & Gould, A. 2004, ApJ, 601, 289

Couteau, P. 1960, J. des Observateurs, 43, 41

De Rújula A., Jetzer P., & Massao E., 1992, A&A, 254, 99

Duquennoy, A. & Mayor, M. 1991, A&A, 248, 485

Gould, A. & Salim, S. 2003, ApJ, 582, 1001

Hartkopf, W. I., & Mason B. D., 2007, Sixth Catalog of Orbits of Visual Binary Stars, WDS06, U.S. Naval Observatory, Washington

Jiang, Y. & Tremaine, S. 2010, MNRAS, 401, 977

Kouwenhoven, M. B. N., Goodwin, S. P., Parker, R. J. et al. 2010, MNRAS,404, 1835

Lepine, S. & Bongiorno, B. 2007, AJ, 133, 889

Lacey, G. C., & Ostriker, J. P. 1985, ApJ, 299, 633

Luyten, W. J. 1979, New Luyten Catalog of Stars with Proper Motions Larger than Two-Tenths of an Arcsecond (Minneapolis: Univ. MinnesotaPress)

Mason, B. D., & Hartkopf, W. I., 2007, IAUS, 240, 575

Mason, B. D., Wycoff, G. L., Hartkopf, W. I. et al. 2001, AJ, 122, 3466

Mason, B. D., Wycoff, G. L., Hartkopf, W.I., 2007, The Washington Double Star Catalog. WDS, U.S. Naval Observatory, Washington

Moeckel, N., & Clarke, C. 2011, MNRAS, 415, 1179

Monroy-Rodríguez, M.A. & Allen, C. 2013, ApJ, in press

Nissen, P. E. & Schuster, W. J., 1991, A&A, 251, 457

Perets, H. & Kouwenhoven, M. B. N. 2012, ApJ, 750, 83

Poveda, A. & Allen, C. 2004, IAU Colloquium 191 - The Enviroment and Evolution of Double and Multiple Stars, Eds. C. Allen & C. Scarfe, RMxAA (SC) 21, 49

Poveda, A., Allen, C. & Hernández-Alcántara, A. 2007, in Binary Stars as Critical Tools & Tests in Contemporary Astrophysics, IAU Symposium 240, Eds. W.I. Hartkopf, E.F. Guinan and P. Harmanec. Cambridge: Cambridge University Press, p. 417

Poveda, A., Allen, C. & Herrera, M. A. 1997, in Visual Double Stars : Formation, Dynamics and Evolutionary Tracks. J.A. Docobo, A. Elipe, and H. McAlister. Dordrecht : Kluwer Academic, ASSL 223, 191

Poveda, A. & Hernández-Alcántara, A. 2003, Stellar astrophysics. Sixth Pacific Rim Conference.Cheng, K. S., Leung, K. C. and Li. T. P. Dordrecht : Kluwer Academic, ASSL 298,111

Poveda, A., Herrera, M. A., Allen, C. et al. 1994, RMxAA 28, 43

Quinn, D. P., Wilkinson, M. I., Irwin, M. J. et al. 2009, MNRAS, 396, 1, L11

Raghavan, D., McAlister, H. A., Henry, T. et al. 2010, ApJS, 190, 1

Reipurth, B. & Mikkola, S. 2012, Nature, 492, 221

Ryan, S. G. 1992, AJ, 104, 1144

Salim, S. & Gould, A. 2003, ApJ, 582, 1011

Sesar, B., Ivezic, Z. & Juri´c, M. 2008, AJ, 689, 1244

Tisserand, P. et al., 2007, A&A, 469, 387

Valtonen, M. 1997, Visual Double Stars : Formation, Dynamics and Evolutionary Tracks. J.A. Docobo, A. Elipe, and H. McAlister. Dordrecht : Kluwer Academic, ASSL. 223, 241

Wasserman, I. & Weinberg, M. D. 1991, ApJ, 382, 149

Weinberg, M. D., Shapiro S. L. & Wasserman I. 1987, ApJ, 312, 367

Wyrzykowski, L. et al., 2009, MNRAS, 397, 1228

Yoo, J., Chanamé, J. & Gould, A. 2004, ApJ, 601, 311

Zapatero-Osorio, M.R. & Martín, E. L. 2004, A&A, 419, 167